Chapter 15A. Summary of the Zarkashan Copper and Gold Area of Interest

Contribution by Stephen G. Peters, Said H. Mirzad, Emily Scott, and Bernard E. Hubbard

Abstract

There are several copper and gold mineral occurrences in the Zarkashan copper and gold area of interest (AOI) in Ghazni Province. Two main study areas are the Bolo gold subarea and the Zarkashan mine subarea. In addition, the Luman-Tamaki gold subarea contains numerous gold prospects. All prospects and the general AOI require detailed mapping and sampling to determine the size and tenor of economic resources at today's gold and copper prices. Sampling by the U.S. Geological Survey (USGS) and the U.S. Department of Defense Task Force for Business and Stability Operations during fiscal year 2010 have substantiated much of the previous Soviet sampling and mapping results and confirmed the presence of copper and gold in concentrations, which indicate that further in-depth evaluation (including geophysics and drilling) would be beneficial. Furthermore, hyperspectral and Advanced Spaceborne Thermal Emission and Reflection (ASTER) radiometer imagery anomalies, newly generated by the USGS, suggest that the distribution of the copper and gold may be extensive and these anomalous zones may define a number of medium- to large-size gold- and copper-rich orebodies that crop out at the surface.

The importance of free gold, identified in many samples, cannot be overemphasized because of widespread distribution of diopside hornfels and (or) skarn in the area and because of the coincidence of these rock types with the hyperspectral anomalies. The gold-rich rocks may be distributed over large areas that could be bulk mined, and the gold ores would be readily amenable to heap leaching using cyanide leach techniques because the bulk of the gold is not refractory.

The Zarkashan potential copper-gold deposits also would be amenable, during early stages of resource development, to simple metallurgical techniques, such as gravity separation, and this would result in short lead times and short payback periods for mining of small- to medium-size gold-copper ore bodies. Initial mining could develop into larger-scale mining owing to the significant future potential of the development of larger orebodies. The area requires additional extensive sampling, compilation, and ground and airborne geophysics as well as drilling and trenching to further outline and test its potential to develop into multiple areas of porphyry copper, large tonnage open pit mines.

15A.1 Introduction

This chapter summarizes and interprets results for the Zarkashan copper and gold area of interest (AOI) and subareas that result from joint geologic and compilation activities conducted from 2009 through 2011 between the U.S. Geological Survey (USGS), the U.S. Department of Defense Task Force for Business and Stability Operations (TFBSO), and the Afghanistan Geological Survey (AGS). Accompanying complementary chapters 15B and 15C address hyperspectral data and geohydrologic assessments respectively of the Zarkashan copper and gold AOI. Additionally, supporting data for this chapter are available from the Afghanistan Geological Survey Data Center in Kabul and include an inventory of individual datasets compiled for the Zarkashan copper and gold AOI and its subareas; the inventory specifies the data that have been compiled.

The Zarkashan copper and gold AOI is located in Ghazni Province in southeastern Afghanistan and includes parts of the Ab-Band, Arghandab, Gelan, Glarabaghn, Jaghuri, and Mokur administrative districts. The area of the main AOI is 1,692 square kilometers (km^2). The three subareas—Luman-

Tamaki gold subarea (356 km^2), Bolo gold subarea (313 km^2), and Zarkashan mine subarea (214 km^2)—are designated as specific prospect areas with a high potential for the presence of commercial mineralized rock (fig. 15A–1).

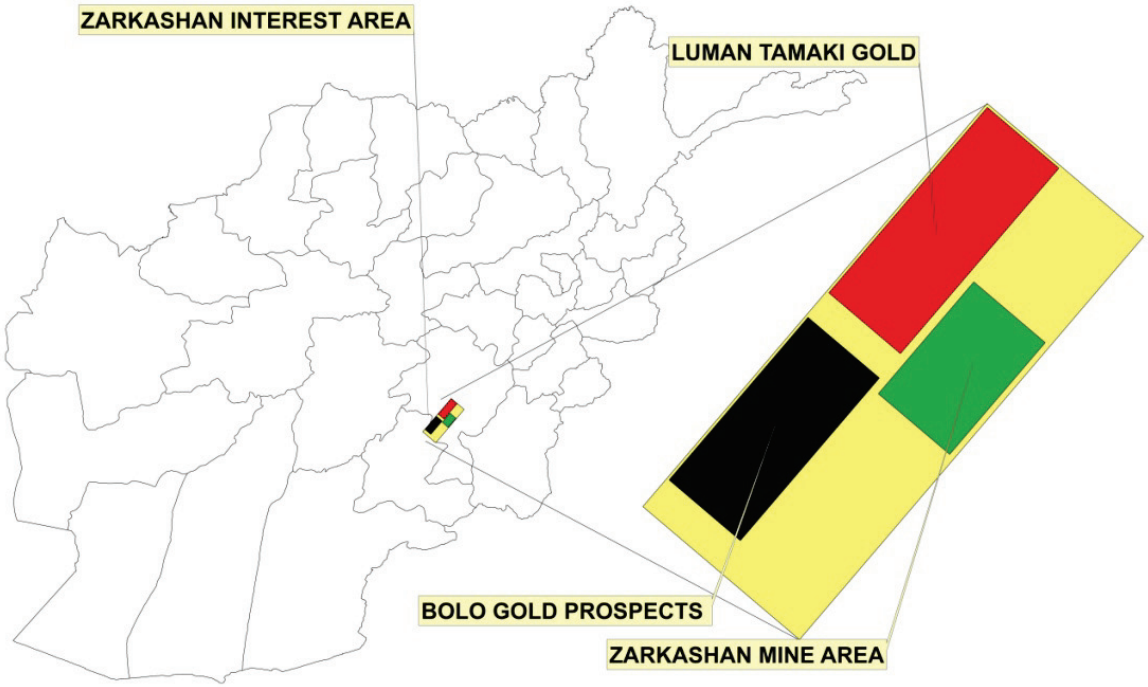

Figure 15A–1. Location of the Zarkashan copper and gold area of interest (yellow) and the three subareas, Luman-Tamaki gold subarea (red), Bolo gold subarea (black), and Zarkashan mine subarea (green).

Mineral deposit types that may be present in the Zarkashan copper and gold AOI are large porphyry copper-gold, and medium-size copper-(gold) skarn, polymetallic vein, iron skarn, and lead-zinc skarn deposits. In addition, placer gold and some tin and tungsten skarn occurrences also are known to be present in the area.

Most existing mineral resource information has been gathered from reports written between the early 1950s and 1985 by geologists from the former Soviet Union who provided Afghanistan with technical assistance. This previous information, combined with a preliminary assessment by the USGS in 2007 (Peters and others, 2007), provided much of the factual basis for the technical work during the 2009 through 2011 scoping mission. The Zarkashan AOI and subareas also were thought to be likely to develop near-term mineral production. In addition, some deposits in the AOI are near-surface bodies with promising metallurgical and mining characteristics.

15A.2 Previous Work

The Zarkashan mine subarea, also called the Mokur gold district, as well as a number of other prospects, have older workings, slag piles, and mill stones that indicate mineral exploitation for copper and gold has been taking place in the area for a long time. The gold placer deposits were described by Homilius (1968, 1970). Early Soviet geological expeditions reported on the gold and copper mineralization in the area (Afghanistan Geological and Mineral Survey, 1967; Khananov and others, 1967; Douvgal and others, 1971; Kononykhin and others, 1971; Kovalenko and others, 1971, Borozenets, 1972). Results of detailed prospecting and sampling and descriptions of many of the individual prospects is given by Meshcheryakov and Borozenets (1970), and Kotov and others (1971). Furthermore, USGS remote sensing work in the region that covers part of the Zarkashan copper and gold AOI was summarized by Sweeney and others (2006; fig. 15A–2), and by Mars and Rowan (2007). Compendiums were assembled by Abdullah and others (1977), United Nations Economic and Social

Commission for Asia and the Pacific (1995), Metal Mining Agency of Japan (1998), Orris and Bliss (2002), Doebrich and others (2006), Ludington and others (2007), and Peters and others (2007) (fig. 15A–3).

A scoping mission was undertaken in the Zarkashan copper and gold AOI on April 18 and 21, 2010, by the USGS and the TFBSO. The landing plan called for visits to the Dynamite (Dynamic), Zardak, and Zarkashan areas in the main Zarkashan mine subarea and to the Belaw, Bolo, and Utkul prospects in the Bolo gold subarea (figs. 15A–1, 15A–2, and 15A–4); all the target areas were visited. The Zardak and Zarkashan areas proved to be well-mineralized in copper and gold, and subsequent analysis of the samples taken confirmed this. The Dynamite area had a different geologic setting than the main Zarkashan mine subarea. The Bolo and Utkul gold prospects were sampled by stream-sediment samples, but the samples taken were from prospective horizons in the streambed and were not representative. In addition to the confirmation of copper and gold at the Zardak and Zarkashan prospects, sampling and mapping during the scoping mission indicated that large areas of hornfels and contact zones around the main Zarkashan intrusion may contain ore-grade copper and gold, which were not sampled or considered by the previous Soviet studies (U.S. Department of Defense Task Force for Business and Stability Operations, 2010).

15A.3 Metallogeny

Porphyry copper and copper-gold deposits are an extremely important source of copper and gold worldwide and are located in plutonic rocks in magmatic arcs in North and South America, Europe, Asia, the southwestern Pacific Ocean, and several other continents. The Tethyan arcs, stretching from the Carpathian Mountains of southern and eastern Europe through East Asia, are the setting for numerous important porphyry copper and copper-gold deposits to the west (Sar Chesmeh, Iran), south (Reqo Diq, Pakistan), and east (Yulong, Tibet) of Afghanistan (Doebrich and others, 2007). Several known copper-bearing occurrences in Afghanistan, including Zarkashan, have measured or indicated copper and gold resources, including the Gbarghey copper skarn [about 70 kilometers (km) north-northeast of Kandahar], the Kundalan copper and gold deposits (about 125 km northeast of Kandahar), and the Shaida copper deposit (about 75 km southwest of Herat) (Abdullah and others, 1977). Regional metallogenesis for porphyry copper and copper-and-gold deposits was summarized by Doebrich and others (2007) who suggested that Triassic, Cretaceous, and Paleocene to Miocene intrusive and volcanic rocks represent areas where porphyry copper and copper-and-gold deposits may exist in Tethyan magmatic arcs in Afghanistan. A synthesis of geologic, mineral deposit, aerogeophysical, remote sensing, and geochemical data for delineated regions permissive for undiscovered porphyry copper deposits is presented in Peters and others (2007). Ludington and others (2007) indicated that the Kundalan, Makran arc, and Zarkashan regions had the highest potential for undiscovered porphyry copper and copper-and-gold deposits. Concealed segments of magmatic arcs in southern Afghanistan, delineated by aeromagnetic data, also represent prospective targets for exploration.

Mineral deposits related to felsic to intermediate porphyritic igneous rocks in Afghanistan include porphyry copper and associated deposits, such as polymetallic skarns and veins and gold-bearing parts of the same systems. The Zarkashan copper and gold AOI is one of a number of areas in Afghanistan that contain mineral occurrences and geologic features that show promise for future discovery and exploitation of these types of large deposits. About 200 igneous-related hydrothermal mineral deposits and occurrences in Afghanistan contain copper as a major commodity. The majority of these are classified as copper skarn (about 50 prospects) and polymetallic vein (about 70 prospects) deposits (Abdullah and others, 1977; Orris and Bliss, 2002; Doebrich and others, 2006). These deposit types typically are associated with and are present in the same geologic environments as porphyry copper and copper-and-gold deposits (Singer and others, 2008; John and others, 2010). Thus, the presence of these deposit types in Afghanistan is evidence that the geologic environments are likely to be permissive for porphyry copper and porphyry copper-and-gold deposits (Doebrich and others, 2007; Ludington and others, 2007).

Because igneous rocks typical of geologic provinces that contain porphyry copper deposits are common in Afghanistan, Ludington and others (2007) and Peters and others (2007) outlined 12 separate magmatic arcs that might contain porphyry copper and porphyry copper-gold and related deposits in the country. Many of these are the same zones summarized by Doebrich and others (2007). Because many of the known porphyry-like prospects are associated with Cretaceous through Late Tertiary plutonic rocks that constitute a number of igneous belts that are part of Tethyan magmatic arcs, many younger, igneous-related copper prospects, like Zarkashan, are located in eastern Afghanistan in the Arghandab, Band-e Bamyan, Chagai, Farah Rod, Helmand, and Spin Boldak plutonic belts northwest of the Chaman fault and south of the Herat fault (Peters and others, 2007).

15A.4 Geology

The geologic setting and regional ore controls of the Zarkashan copper and gold AOI are different in the northwestern and southeastern parts (figs. 15A–2 and 15A–3). The northwestern parts of the Zarkashan copper and gold AOI that contain the Bolo gold subarea consist of Late Proterozoic metamorphic rocks and Lower Paleozoic dolomite, limestone, and shale and Carboniferous to Early Permian mafic volcanic rocks, sandstone, shale, and siltstone, all intruded by parts of the Oligocene Arghandab Phase I granodioritic batholiths rocks (Kotov and Mecherjakov, 1970; Doebrich and others, 2006: Peters and others, 2011). The rocks are intruded in the Bolo gold subarea and the Zarkashan mine subarea by the Zarkashan suite of intrusive bodies (fig. 15A–4), which are composite Late Cretaceous to Paleocene adamellite, diorite, gabbro, and granodioritic stocks and plutons. This suite has a unique magnetic expression (fig. 15A–1).

The central and eastern parts of the Zarkashan copper and gold AOI comprise a sequence of Permian to Triassic calcareous rocks that are overlain unconformably by Cretaceous limestone and sandstone. The intrusive rocks are petrologically and metallogenically distinct from granitic rocks of the Oligocene Arghandab batholith. The main copper- and gold-mineralized areas in the Zarkashan copper and gold AOI are related to the Zarkashan pluton, which is reflected as positive anomalies in the aeromagnetics (fig. 15A–1).

15A.5 Known Deposits and Prospects

Two subareas in the Zarkashan copper and gold AOI (figs. 15A–1, 15A–2, and 15A–3), the Bolo gold and the Zarkashan mine subareas, are considered most favorable by Peters and others (2007). Both subareas contain known and partially explored prospects with potentially economically important gold contents. Development of small- to medium-sized, high-grade gold deposits typically could be accomplished in a far shorter time frame than porphyry copper prospects (table 15A–1). The main Zarkashan copper and gold AOI and the Luman-Tamaki gold subarea (fig. 15A–4) also contain gold prospects that may have promise for future development, but are not as well documented.

The Bolo gold subarea lies along the west margin of the Zarkashan copper and gold AOI along a linear alignment of gold-copper skarn, vein, and unclassified gold occurrences that are associated with Cretaceous or Paleogene diorite dikes and small intrusive bodies (figs. 15A–5 and 15A–6*a*). These gold occurrences are hosted in Upper Permian carbonate rocks. The gold-bearing skarn occurrences contain mineralized rock with as much as 35 grams per metric ton (g/t) gold (Khananov and others, 1967; Meshcheryakov and Borozenets, 1970; Douvgal and others, 1971; table 15A–1). Gold-bearing veins and potential gold placer deposits also are present (figs. 15A–6*a* and *b*).

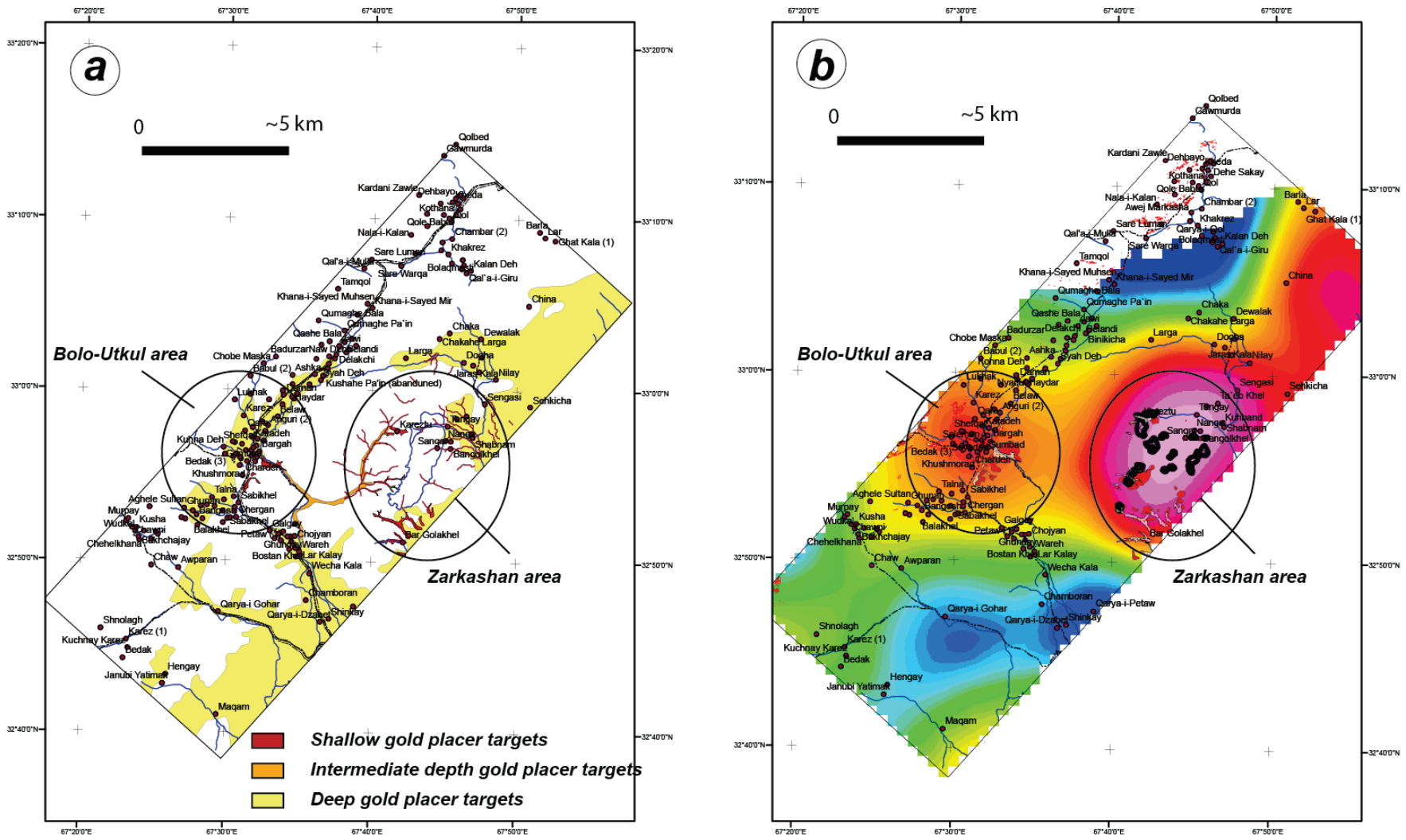

Figure 15A–2. Maps showing the locations of the Bolo gold and the Zarkashan mine subareas. (*a*) Location of the two subareas (ellipses) showing major areas of gold placer potential. (*b*) Location of the two areas superimposed on the aeromagnetic anomaly map by Sweeney and others (2006). Anomalous zones are shown in dark outline. Small annotated dots are individual villages.

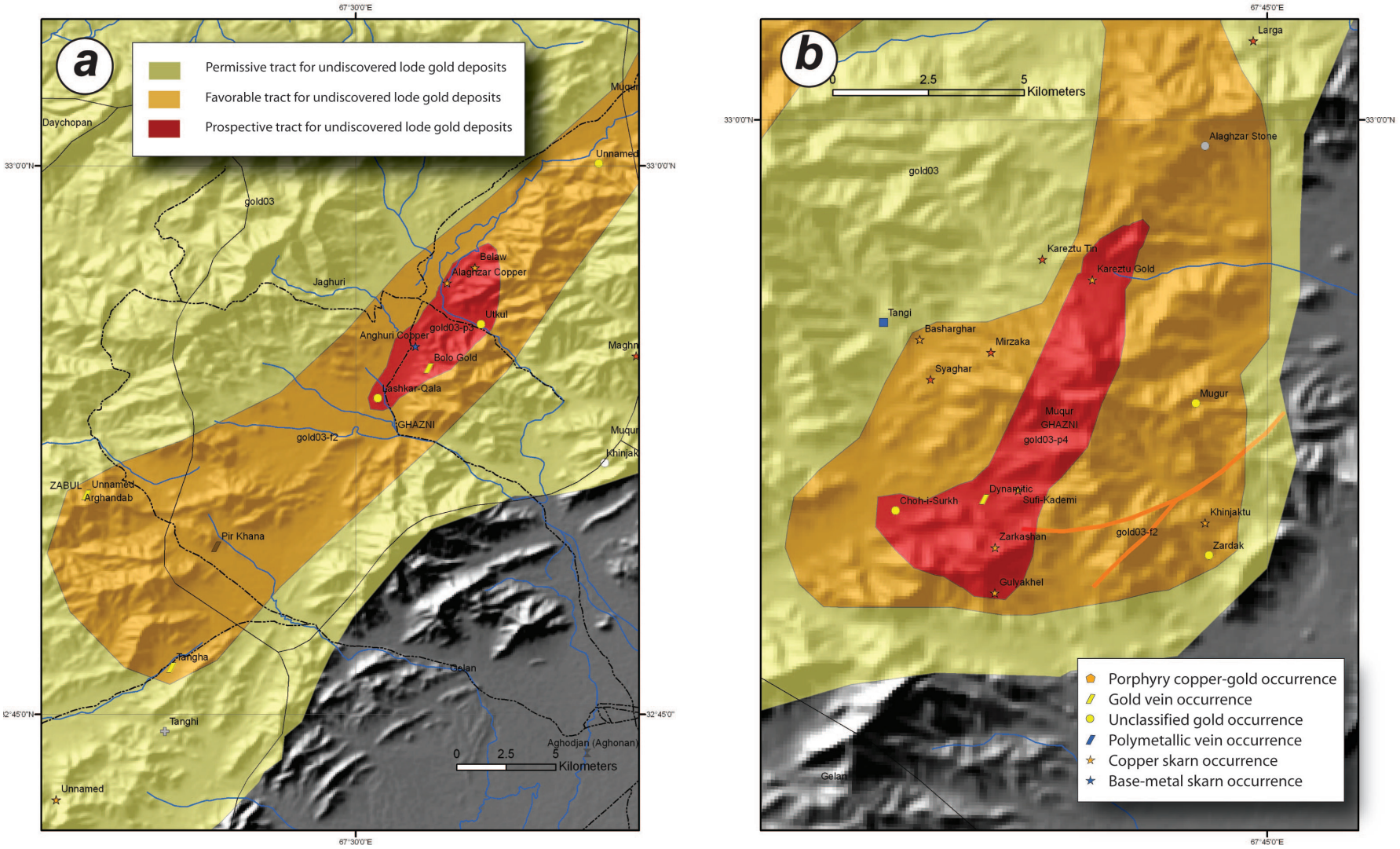

Figure 15A–3. Maps showing location of the region around the Zarkashan copper and gold area of interest from Peters and others (2007). (*a*) Assessment map showing areas of potential and main prospects in the Bolo gold subarea. (*b*) Assessment map showing areas of potential and main prospects in the Zarkashan mine subarea.

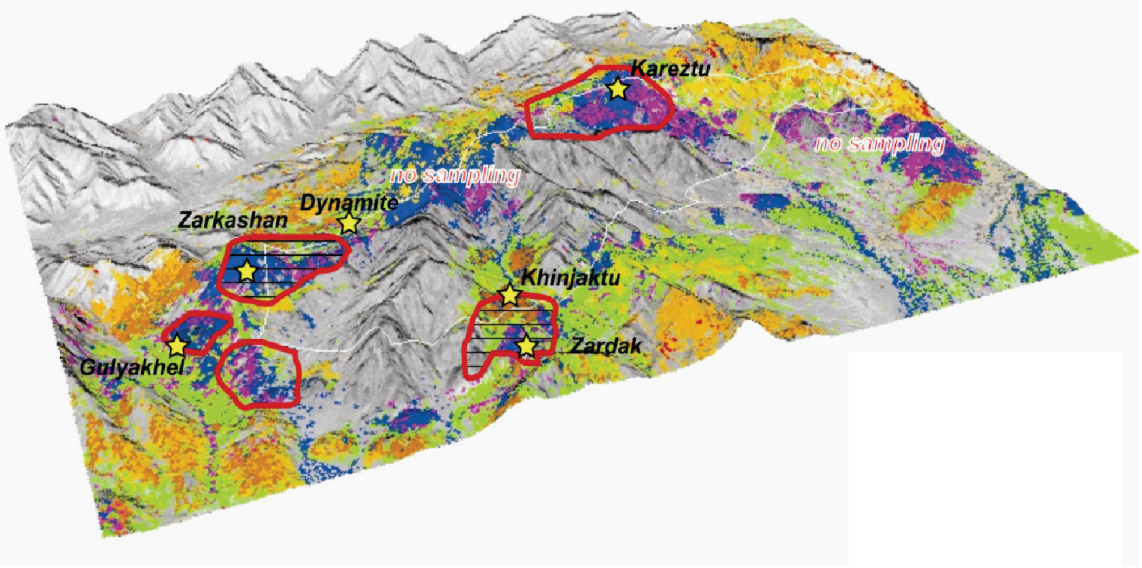

Figure 15A–4. Three-dimensional view of the Zarkashan copper and gold area of interest showing hyperspectral anomalies surrounding the Zarkashan intrusive (white outline). The blue and purple zones represent alteration zones with goethite and jarosite. These alteration zones also are coincident with anomalous gold areas from sampling reported in Kotov and Mecherjakov (1967). Additionally, two of these zones were visited and sampled by the scoping mission of the U.S. Geological Survey and the U.S. Department of Defense Task Force for Business and Stability Operations during 2010, which confirmed the presence of copper and gold in abundance. Six of the anomalous areas contain known gold occurrences or deposits (Abdullah and others, 1977).

In the Zarkashan mine subarea, in the eastern part of the Zarkashan copper and gold AOI, a number of other skarn occurrences form a north-trending, roughly 5–km-wide zone along the west and east margins of the Zarkashan Cretaceous to Paleogene pluton (fig. 15A–5). The host country rocks are Triassic carbonate rocks and mudstone sequences. A number of mineralized zones are present in and around the northeast-elongated granodioritic Zarkashan pluton. The skarns (Dynamite, Guyakhel, Khinjaktu, Sufi-Kademi, Zardak, and Zarkashan) are all gold-bearing (table 5A–1). They are part of four main target zones in the subarea, the Guyakhel, Kereztu gold, Khinjaktu-Zardak, and Zarkashan-Dynamite target zones, that have been delineated on the basis of geochemical sampling and recent hyperspectral and ASTER mapping of anomalous zones (figs. 15A–6*a* and *b*). Several other mineral occurrences in the area (Kereztu tin, Maghn, Mirzaka, and Syaghar) are classified as tin skarn (Doebrich and others, 2006), and cassiterite is the most abundant ore mineral in those occurrences. Although these tin and tungsten prospects potentially have important copper contents (Abdullah and others, 1977; Doebrich and others, 2006), they are most likely related to intrusive activity associated with the Arghandab Batholith and are not part of the gold-bearing Zarkashan igneous suite (Peters and others, 2007).

The Zarkashan copper-gold deposit and peripheral zones, alteration anomalies, and targets comprise copper and gold mineralization in skarn and in shattered zones that contain areas with

alteration phases resulting from serpentinization, silicification, and carbonatization. The skarns are garnet-vesuvian-diopside and diopside-bearing types. They also contain epidote, phlogopite, and wollastonite. The principal ore minerals are bornite, chalcocite, chalcopyrite, native gold, pyrite, and sphalerite. These ore minerals are present in massive sulfide pods or are finely and irregularly disseminated throughout the country rock. Several auriferous zones were delineated by Soviet studies where various orebodies were defined. The gold content in the pods varies from several fractions of a gram to 10 g/t gold. The tenor of gold in the Zarkashan mine and at the Zardak gold occurrence was confirmed in 2010 by the USGS and the TFBSO (U.S. Department of Defense Task Force for Business and Stability Operations, 2010).

Gold in the skarns of the Zarkashan copper and gold AOI is spatially associated with calcite, copper sulfide minerals, quartz, and serpentine. The richest chalcopyrite and gold ore is found in phlogopite skarn. Mineralization of the high-grade ores is extremely irregular, and therefore these orebodies are not persistent along strike and dip. Gold content measured by Soviet studies in the high-grade skarn pods varies from "traces" to 245 g/t gold, and that of copper, from 0.01 to 15 weight percent (wt. %) copper. Cadmium, lead, molybdenum, and zinc also are present in minor quantities (table 15A–1).

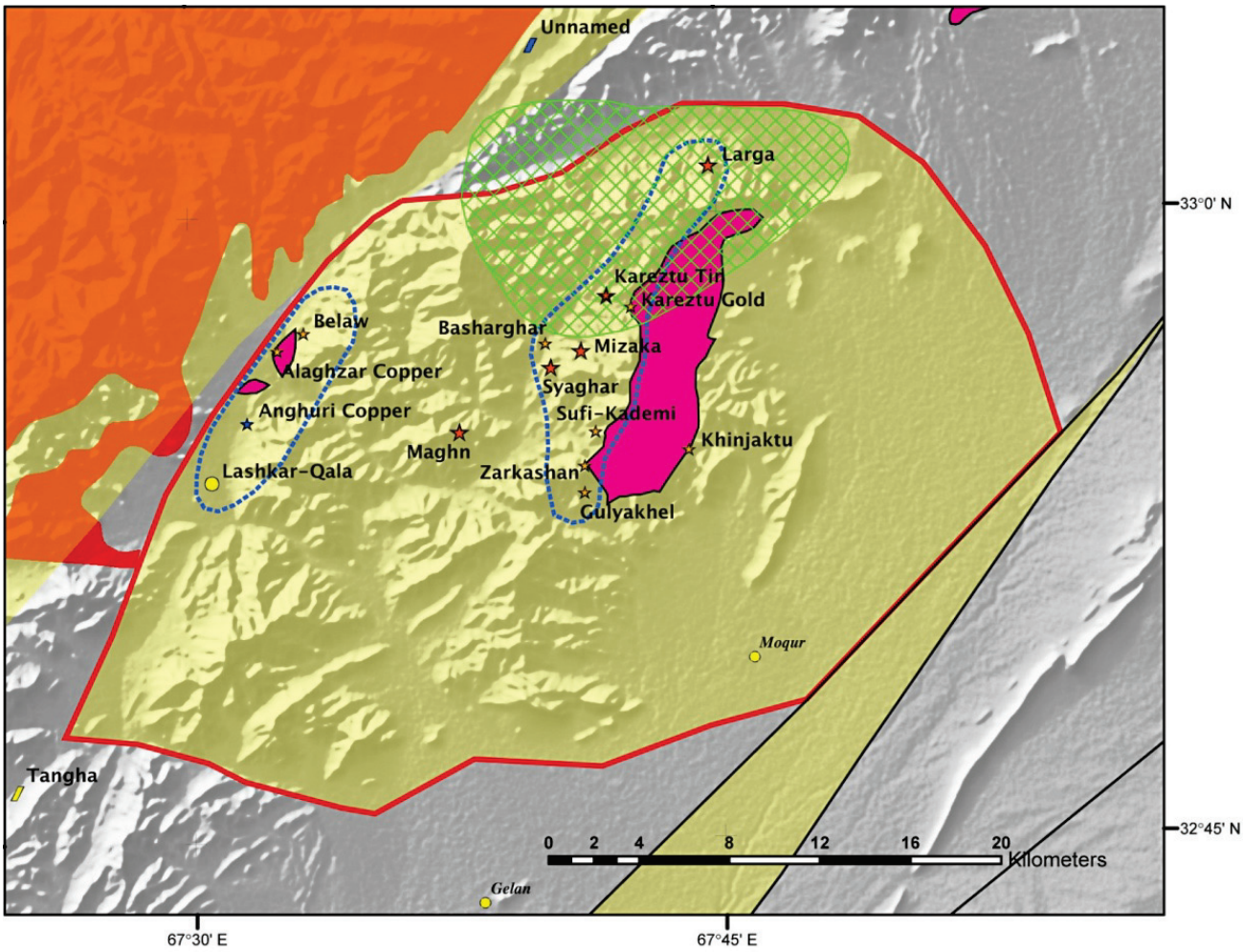

Figure 15A–5. Map of the Zarkashan copper and gold area of interest (outlined in red), which is part of the Kundalan Zarkashan porphyry copper-gold permissive tract of Ludington and others (2007). Alkaline Cretaceous to Paleogene Zarkashan suite intrusive rocks are shown in pink (map unit KP_1gbm of Doebrich and others, 2007). Green crosshatch is a tin mineral halo. Blue dashed lines outline the most favorable parts of the permissive tract (Peters and others, 2007); the two areas outlined are parts of the Bolo gold subarea in the west and the Zarkashan mine subarea in the east.

Table 15A–1 Prospects in the Zarkashan cooper and gold area of interest.

[Gold grades and dimensions in two subareas are also included. Data are from Abdullah and others (1977). Au, gold; Cu, copper; g/t, gram per metric ton; m, meter; Zn, zinc]

Subarea	Prospect	Size, surface dimensions (m)	Gold grade (g/t Au)	Comments
Bolo gold	Belaw	2–25 × 250	0.1–0.8	Skarn, limonite 1 to 4 g/t Au.
Bolo gold	Alaghzar	70–100 × 500	0.01–1.6	As much as 35 g/t Au in serpentine.
Bolo gold	Bala	0.5–12 × 140	0.8–34	Fault zone with limonite.
Bolo gold	Anguray	1–10 × 189	0.3–142	Skarn zone with Cu and Zn.
Bolo gold	Utkul	0.5 × 300	<11	Fault zone with limonite.
Bolo gold	Bashargar	1 × 50–80	2.9–12.3	43 g/t Au in limonite.
Zarkashan mine	Khinjaktu	200	1.8	Skarn.
Zarkashan mine	Zardak	50–140 long	1.2–19.4	Skarn igneous breccias.
Zarkashan mine	Guyakhel	1.5 × 50 × 70	4.4	Skarn.
Zarkashan mine	Sufi Kademi	Skarn beds with conglomerate	7	Ancient workings.
Zarkashan mine	Dynamite	0.6–1.2	4–70	Drill holes, ancient workings.
Zarkashan mine	Chah-i Surkh	0.2–2.5 × 100	0.6–3.2	Shattered limonite zone.

15A.6 Economic Geology

The Zarkashan copper and gold AOI contains a number of mineralized zones. The most well known and well studied is the Zarkashan mine in the Zarkashan mine subarea, which consists of a number of skarn zones along the western and eastern contacts of the Zarkashan pluton (fig. 15A–6*a* and *b*).

The Zarkashan mine subarea skarn deposits result from a Late Cretaceous to Paleocene adamellite, diorite, and granodiorite as well as pluton rocks that have intruded into Upper Jurassic to Lower Cretaceous limestone, sandstone, and siltstone (fig. 15A–6*a*). Mineralized garnet-magnetite-vesuvianite-wollastonite-diopside skarn zones contain bornite, chalcopyrite, covellite, native gold, and pyrite (Abdullah and others, 1977; Orris and Bliss, 2002). Pyrite-chalcopyrite mineralized rock spatially is associated with amphibole, garnet, magnetite-pyroxene-garnet-phlogopite, phlogopite, phlogopite-pyroxene, pyroxene, pyroxene-garnet, and pyroxene-magnetite skarns. The largest concentrations of sulfide minerals are present in the magnetite-pyroxene-garnet-phlogopite and phlogopite-magnetite skarns. In addition to chalcopyrite, magnetite, and pyrite, the skarns also contain molybdenite, sphalerite, and tetrahedrite. Bismuth, gold, and silver are typical accessory elements associated with skarn (Kotov and others, 1970).

Samples collected in 2010 by the USGS and the TFBSO were examined by standard petrographic methods, followed by a study using the scanning electron microscope (SEM) (figs. 15A–7 through 15A–12) at the Menlo Park, Calif., USGS facility (Theodore, 2010). The SEM study was conducted primarily because of the high content of gold in a number of samples from Zarkashan and recognition of free gold in four of the polished thin sections examined (sample nos. ZR10010C, ZR10015A, and ZR10015B; table 15A–2).

The skarns contain prograde silicate phases in the garnet-pyroxene skarn. Garnet is mostly isotropic grossularite (fig. 15A–7). However, minimal amounts of more iron-rich (and anisotropic) varieties are present, mainly as late-stage precursors on the margins of the grossularite. A presulfide lining to open cavities that subsequently were filled by chalcopyrite (now oxidized) also is present, as are two generations of diopside, early-stage stubby diopside crystals (many pre-grossularite) and a late prograde-stage acicular or more fibrous diopside that is later than the stubby diopside. Some trace amounts of actinolite also are present. The garnet (grossularite)-pyroxene (diopside) skarn usually includes some fairly large clots of 1.5–centimeter (cm)-wide frothy iron oxide as a result of weathering (Theodore, 2010).

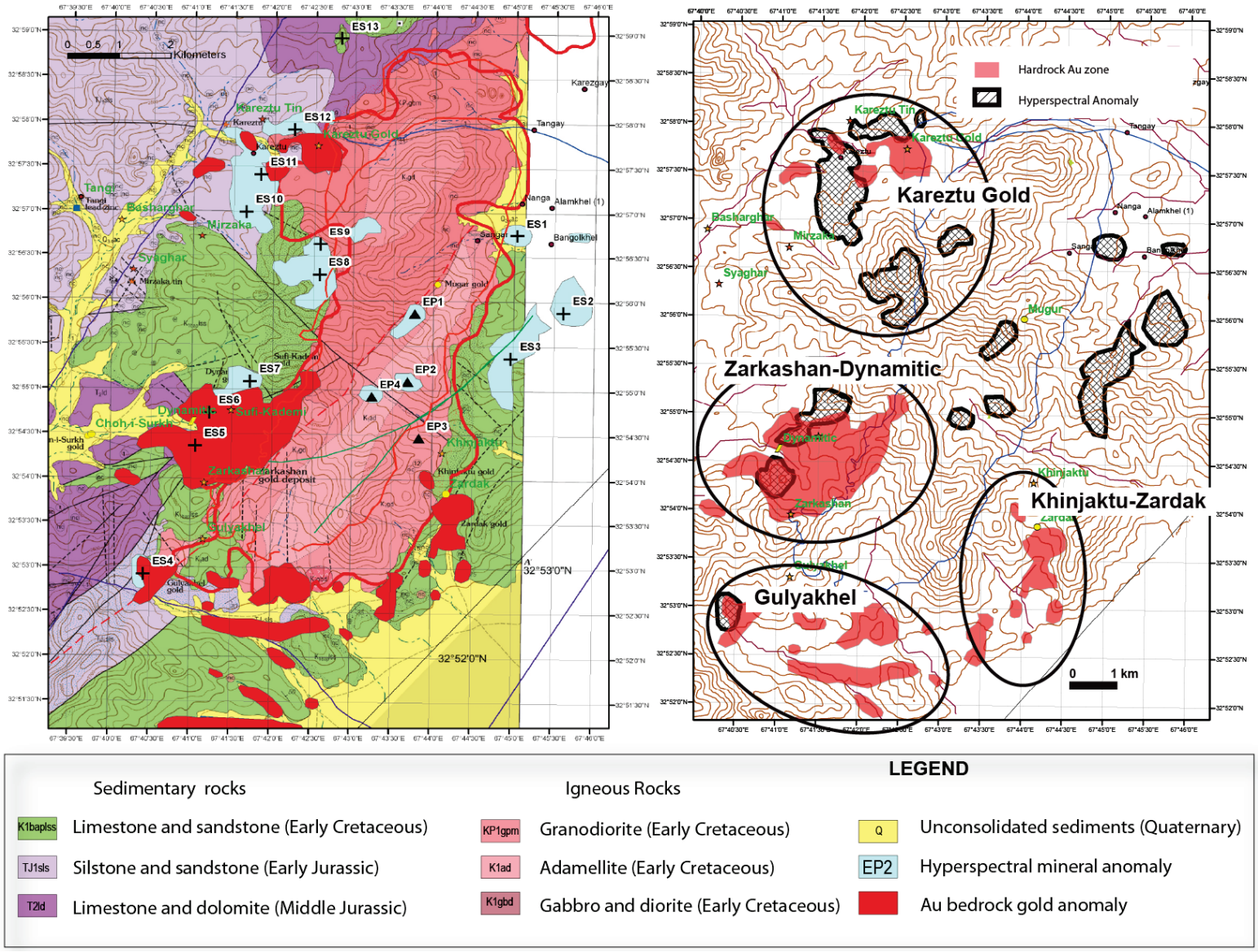

Figure 15A–6. Maps showing mineralized areas and targets around the Zarkashan pluton in the Zarkashan mine subarea of the Zarkashan copper and gold area of interest. (*a*) Portion of geologic map of Zarkashan (adapted from Peters and others, 2011) showing target areas. (*b*) Topographic map showing target areas (in ellipses), hyperspectral anomalies (cross-hatch areas), and bedrock gold anomalous zones (red shade).

Table 15A–2. Gold concentrations for several grab rock samples taken from the Zarkashan mine subarea in 2010.

[Analysis performed by the U.S. Geological Survey laboratory in Denver, Colo. Some samples are shown in figure 15A–16. Au, gold; ppb, parts per billion]

Lab no.	Field no.	Sample description	Au, in ppb
C–341562	ZR100001	pyrrhotite sericite in hornfels	11,000
C–341563	ZR100002	malachite-stained skarn	9,460
C–341564	ZR100003	slate and malachite and chalcopyrite	1,770
C–341565	ZR100004	malachite-stained skarn and greisen	23,000
C–341566	ZR100005	malachite and skarn/slate	182,000
C–341567	ZR100006	black malachite-stained skarn	18,000
C–341568	ZR100007	pyrite-rich sericite hornfels	6,800
C–341569	ZR100008	sericite-hornfels	6,400
C–341570	ZR100009	pyrite-rich skarn	70,000
C–341571	ZR100010	oxidized ore and pyrite	8,490
C–341572	ZR100011	oxide ore	13,000
C–341573	ZR100012	malachite-stained hornfels	35,000
C–341574	ZR100013	malachite-stained hornfels	88,000
C–341575	ZR100014	fibrous hematite	533
C–341576	ZR100015	hornfels (background)	19,000
C–341577	ZR100016	malachite-stained hornfels	1,290
C–341578	ZR100017	pyrite-rich hornfels/skarn	11,000
C–341579	ZR100018	malachite-stained hornfels	6,240

Diopside- and sparse garnet-bearing marble is flooded by sulfide minerals and micas. Also, centimeter-wide clots of fine-grained biotite are dotted throughout by small crystals of clinopyroxene (diopside). However, textural relations suggest that the biotite clots are older than crystallization of the surrounding phlogopite—the biotite clots also contain no sulfide minerals. The biotite clots probably represent a shaly premetamorphism fraction, originally within limestone, which was then converted largely to biotite and diopside during contact metamorphism, and subsequently was altered marginally to phlogopite during introduction of pyrrhotite and chalcopyrite. Phlogopite along margins of the biotite clots is postbiotite.

Most marble is flooded by green-colored phlogopite and sulfide minerals as well as tetradymite, which is widespread, typically in interstices among well-formed blades of phlogopite or on margins of either chalcopyrite or pyrrhotite. Sulfide minerals and phlogopite were introduced together (figs. 15A–7 and 15A–11).

Massive replacement of marble by pyrrhotite [about 40 volume percent (vol. %)] and phlogopite is common, but some pyrrhotite is secondarily altered to bird's eye texture (fig. 15A–7). Phlogopite is altered marginally to chlorite. Relict calcite from the replaced marble is sparse.

High abundances of vesuvianite are present in some skarn. Growth zones of almost isotropic and low birefringent vesuvianite indicate a fluctuation of major-element ratios in fluids associated with its crystallization just prior to cessation of its growth (fig. 15A–7*c*). In addition, some open spaces prior to introduction of sulfide minerals and gold are partly filled by potassium-feldspar, something common in many similar copper-gold skarns in other parts of the world (Theodore, 2010).

15A.7 Characteristics of the Copper and Gold Ores

The bulk of the gold at the surface of the Zarkashan mine subarea is hosted by iron oxide minerals resulting from oxidation of chalcopyrite that is present in the cores of some of the iron oxide minerals. The bismuth phase that may mantle the gold is later than the gold and probably is paragenetically related to the breakdown of chalcopyrite to iron oxide. Tetradymite also is present as an open space filling among garnet crystals (figs. 15A–8 through 15A–11).

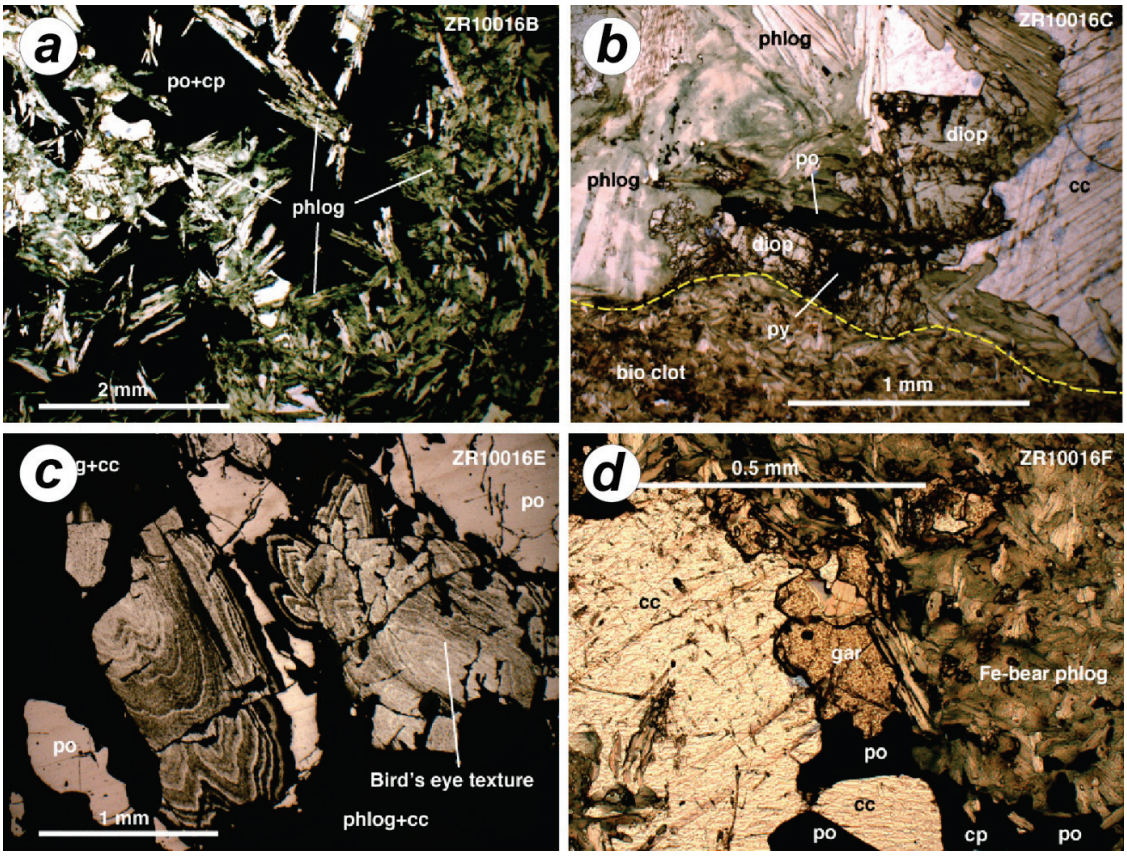

Figure 15A–7. Back-scattered electron micrographs and petrographic microscope images of skarn (adapted from Theodore, 2010). (*a*) Sample ZR10016B marble flooded by phlogopite and minor siderite. Small grains of tetradymite are scattered through the polished thin section (not visible in transmitted light) (*b*) Sample ZR10016C, a diopside- and sparse garnet-bearing skarn with sulfide minerals and fine-grained biotite. (*c*) Sample ZR10016E, a massive replacement of marble by pyrrhotite (about 40 volume percent) with chalcopyrite, sparse molybdenite, phlogopite, and tetradymite present. (*d*) Sample ZR10016F, a biotite hornfel locally recrystallized to marble, including garnet (gar) between phlogopite and pyrrhotite. cc, chalcocite; cp, chalcopyrite; diop, diopsite; Fe-bear, iron-bearing; mm, millimeters; µm, micrometer; phlog, phlogopite; po, pyrrhotite.

Free gold, as well as the bismuth-tellurium mineral tetradymite and additional bismuth-only phases (native bismuth or bismite) also are present. Though the overwhelming bismuth phase in the rock originally was sulfur-free tetradymite (Bi_2Te_3), some bismuth-only phases (bismuth being the only metal present) also have been found—either native bismuth or bismite, mostly in iron oxide. Bismuth-bearing phases and gold rarely are in direct contact. Well crystalline, euhedral gold is partly mantled by native bismuth or bismite, and the gold and bismuth phases are included in much more laterally expansive iron oxide (fig. 15A–9*d*).

In addition, bismuth (as native bismuth or bismite) is present along the margins of some of the iron oxide and mixed chrysocolla-covellite clots. Some fairly well crystalline vesuvianite is concentrated preferentially near many of the iron oxide concentrations as well (figs. 15A–9 and 15A–10).

The gold-to-silver ratio of many gold blebs in figure 15A–10*a* and *b* is about 5:2, on the basis of energy-dispersive X-ray spectroscopy peak heights for each of the two elements. Free gold in the sample also is present as a number of small blebs in open spaces among diopside crystals. The textural relations also suggest chalcopyrite, diopside, gold, the scapolite-group mineral meionite, and sphene may have been coexisting stably at one time prior to secondary alteration of much of the chalcopyrite to chalcocite. Although not much meionite is present in the rock, where it is present, it is in close textural association with unaltered chalcopyrite.

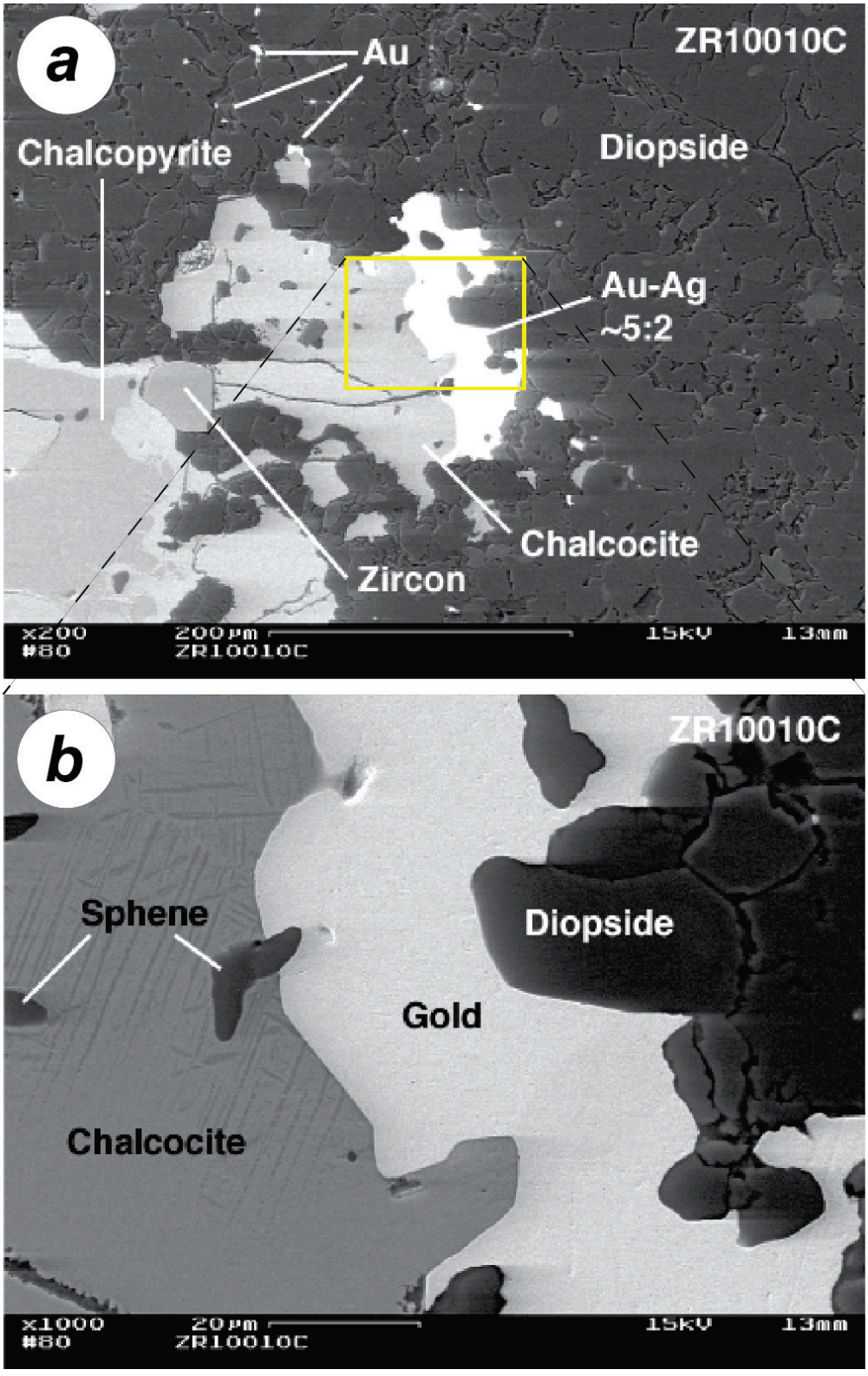

Figure 15A–8. Back-scattered electron micrographs of sample ZR10010C (adapted from Theodore, 2010). (*a*) Chalcopyrite-bearing cogenetic diopside-quartz skarn contains widespread concentrations of the scapolite group mineral meionite and a 200-micrometers (µm)-wide irregularly shaped bleb of free gold. (*b*) A close-up view of the central part of the gold bleb (inset in *a*) shows in remarkable detail this particular bleb. The numbers along the bottom are, from left to right, magnification, scale bar in micrometers, kilovolts used, and working distance, in millimeters (table 15A–2). Ag, silver; Au, gold; kV, kilovolt; mm, millimeter; µm, micrometer.

Shaly limestone is converted to a biotite hornfels, and the limy parts are recrystallized to marble prior to circulation of skarn-sulfide mineral related fluids. Most zones contain tetradymite but may also include some gold-telluride minerals as late phases along crystal edges between phlogopite and pyrrhotite (fig. 15A–12). Additional sulfide minerals include chalcopyrite and extremely sparse molybdenite, and 5-micrometer (µm)-size uranium-thorium oxide minerals adjacent to some zircon are also present in the polished thin section.

The relative amount of large gold blebs compared to the amount of sulfide minerals argues against the gold being a solid solution in chalcopyrite and then being released as free gold during conversion of chalcopyrite to chalcocite (fig. 15A–13). Free gold most likely formed with chalcopyrite (Theodore, 2010). Some interstices among diopside crystals are now occupied by chlorite and kaolinite, which are produced during the conversion of chalcopyrite to chalcocite (fig. 15A–13). Chalcocite, therefore, is most likely genetically associated with chlorite, the iron oxide minerals, and kaolinite. In addition, pseudohexagonal twin traces common in chalcocite are readily apparent and grains of sphene are present in chalcocite and straddle the gold-chalcocite contact, whereas, sphene and diopside are part of the same compatibility elsewhere in the rock (fig. 15A–9*a*).

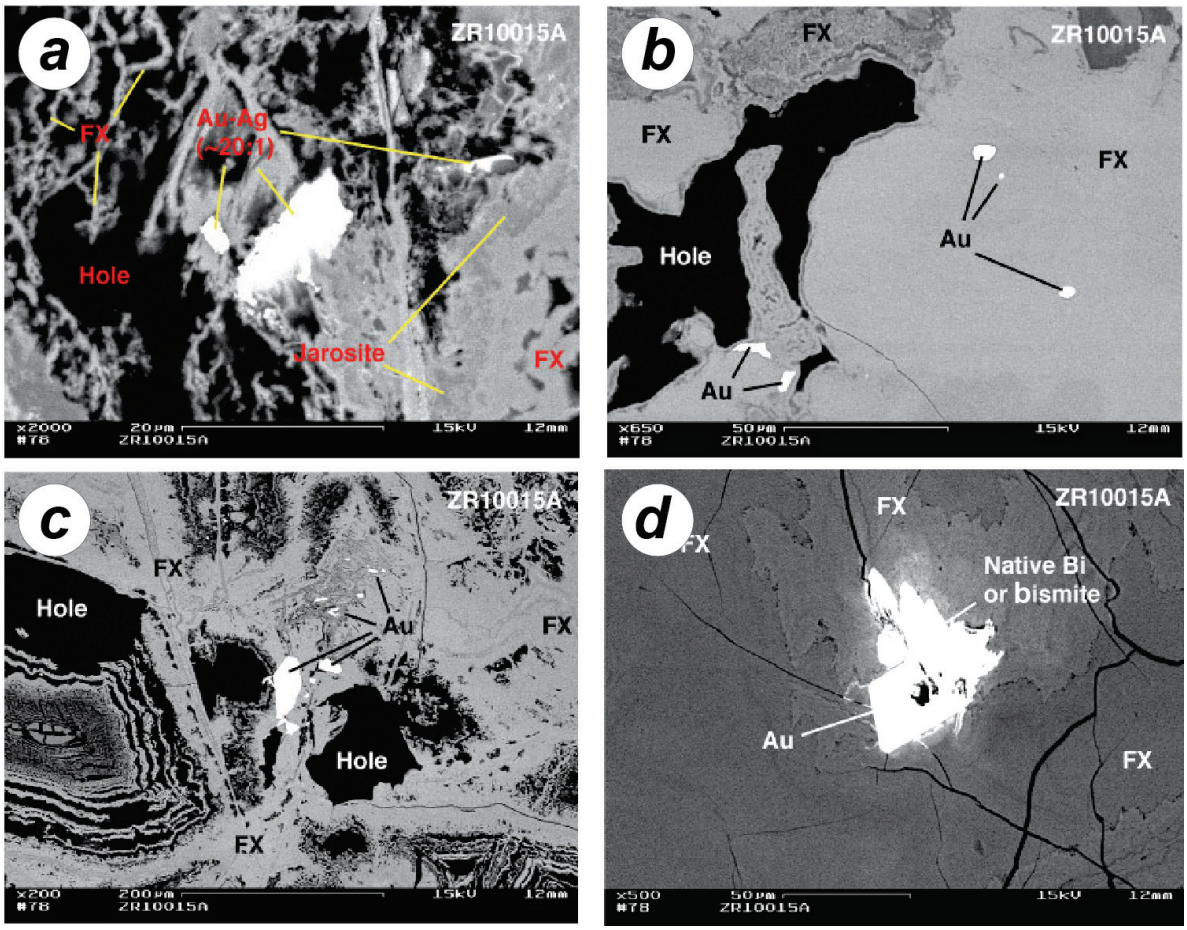

Figure 15A–9. Back-scattered electron micrographs of sample ZR10015A, showing free gold in iron oxide minerals. The gold-to-silver (Au:Ag) ratios in the blebs of gold in this sample are on the order of approximately 20:1 to 10:1, based on a small number of determinations. In addition, some iron oxide zones also contain jarosite (adapted from Theodore, 2010). (*a*) Free gold is contained in iron oxide minerals (FX) and jarosite. (*b*) Free gold contained within iron oxide minerals. (*c*) Free gold within iron oxide minerals and zoned former sulfide grain. (*d*) Bismuth phase mantling gold and oxidized chalcopyrite. The numbers along the bottom are, from left to right, magnification, scale bar in micrometers, kilovolts used, and working distance, in millimeters (table 15A–2). Bi, bismuth; kV, kilovolt; mm, millimeter; µm, micrometer.

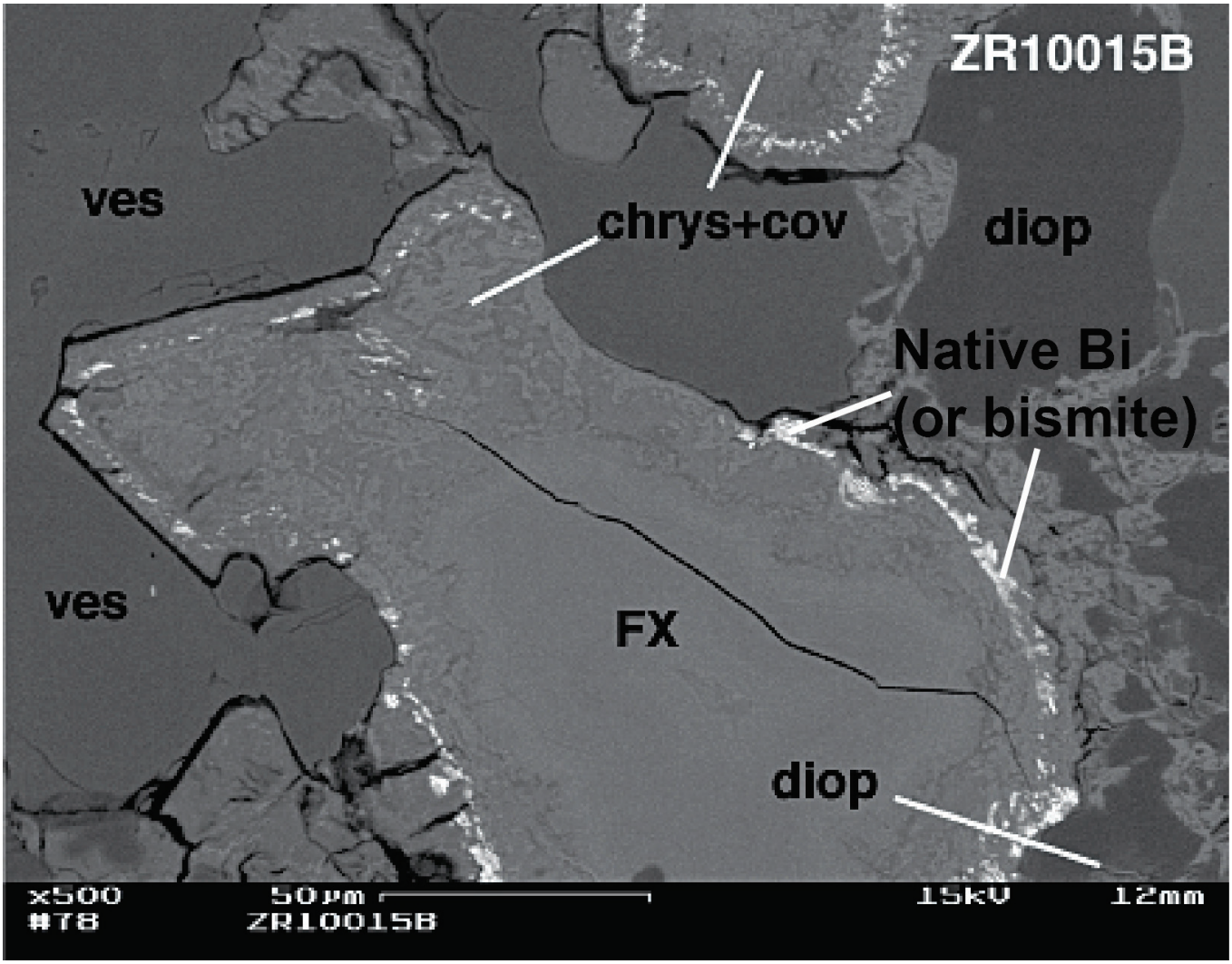

Figure 15A–10. Back-scattered electron micrograph of sample ZR10015B, a grossularite-diopside copper (chalcopyrite)-gold skarn, along margins an iron oxide and mixed chrysocollA-covellite clot (adapted from Theodore, 2010). Crystalline vesuvianite also is concentrated adjacent to iron oxide concentrations. The numbers along the bottom are, from left to right, magnification, scale bar in micrometers, kilovolts used, and working distance, in millimeters (table 15A–2). Bi, bismuth; chrys, chrysacolla; cov, covellite, diop, diopsite; kV, kilovolt; mm, millimeter; µm, micrometer; ves, vesuvianite.

15A.8 Zarkashan Mine Subarea

The Zarkashan copper and gold mine deposit and peripheral zones and targets (Dynamite, Chah-i-Surkh, and Sufi Kademi prospects) comprise gold and copper mineralization in skarn and shattered zones around a small satellite boss west of the main Zarkashan intrusive (fig. 15A–14). In the clastic rocks, the Zarkashan target zone is marked by red color anomalies in the mudstone (fig. 15A–15*a*). The skarns are garnet-diopsite-vesuvian and diopside types and also contain epidote, phlogopite, vesuvianite, and wollastonite. The principal ore minerals are bornite, chalcocite, chalcopyrite, native gold, pyrite, and sphalerite, which are present in massive sulfide pods or are finely and irregularly disseminated throughout the country rock (fig. 15A–16).

Several auriferous zones were delineated by Soviet workers in the Zarkashan mine subarea, and this work defined various orebodies that were from 1 to 15 meters (m) wide with strike lengths of 10 to 600 m. These orebodies are described as lenses that are from 1.5 to 50 m long and 0.5 to 3.8 m thick. Gold concentrations in these orebodies vary between several tenths and 10 g/t gold. The zones were

defined by trenching at the surface followed downward by tunneling (fig. 15A–15*b*) and drilling to a depth of 80 m. The category C_1 and C_2 reserves are 7.7 metric tons (t) of gold (Abdullah and others, 1977). The tenor of gold and copper in the Zarkashan mine subarea and at Zardak prospect area reported by Soviet and Afghan geologists was confirmed in 2010 by the USGS and TFBSO scoping mission (table 15A–2; U.S. Department of Defense Task Force for Business and Stability Operations, 2010). A number of streams that drain the area have potential for small-sized gold placer deposits (figs. 15A–14*a,b*; Homilius, 1968, 1970).

The Chah-i-Surkh prospect within the Zarkashan-Dynamite target zone (figs. 15A–6 and 15A–14) lies along a shattered zone, 0.2 to 2.5 m wide and 100 m long, that is in slightly marmorized limestone of Middle Triassic age and mineralized by hematite and limonite, assaying 0.6 to 3.2 g/t gold (Meshcheryakov and Borozenets, 1970).

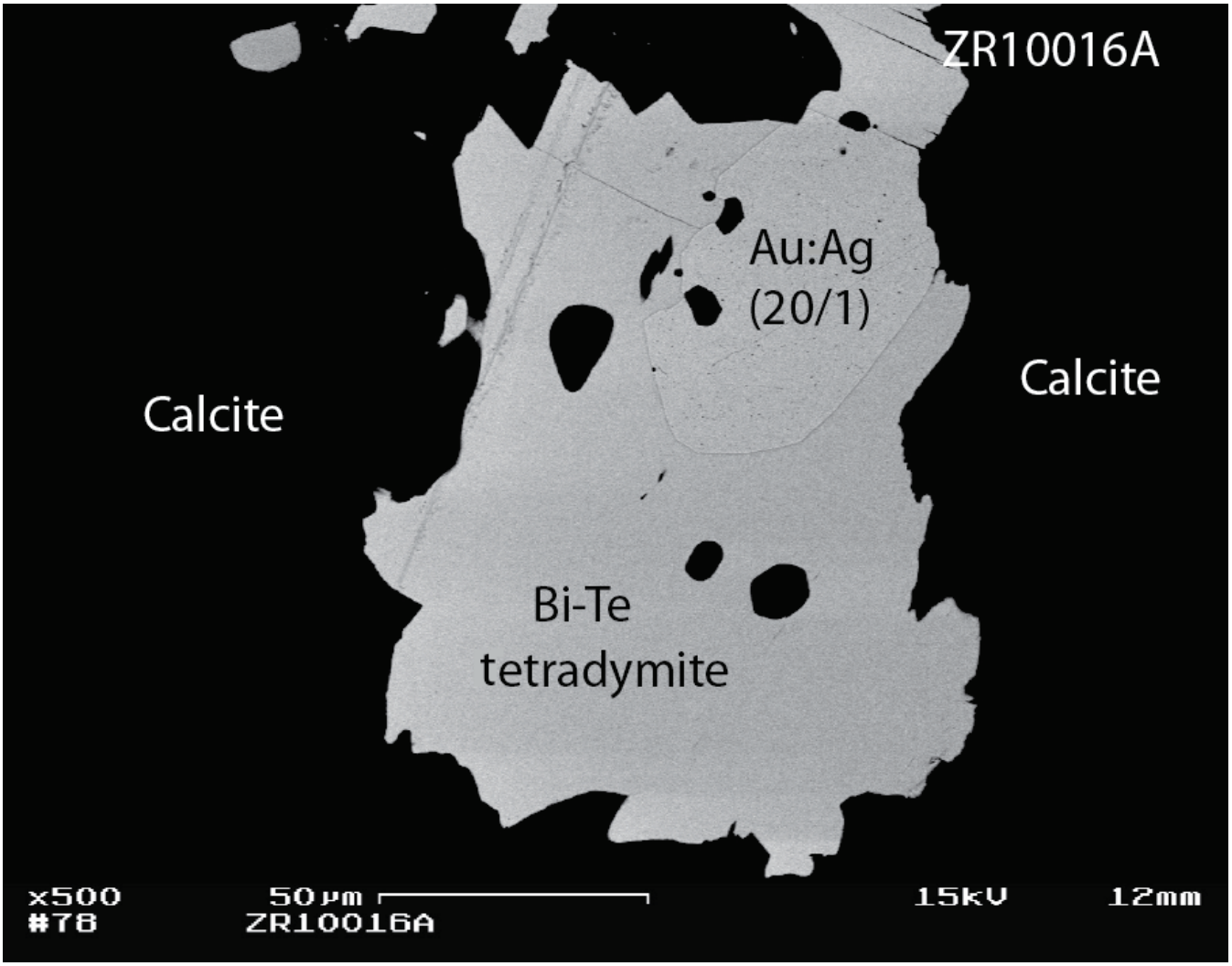

Figure 15A–11. Back-scattered scanning electron micrograph of sample ZR10016A, a marble flooded by sulfide minerals (adapted from Theodore, 2010). Calcite is associated with introduction of chalcopyrite, pyrrhotite, and bismuth-tellurium tetradymite. Textural evidence for direct replacement of calcite by gold and tetradymite also is present. The numbers along the bottom are, from left to right, magnification, scale bar in micrometers, kilovolts used, and working distance, in millimeters (table 15A–2). Ag, silver; Au, gold; Bi, bismuth; kV, kilovolt; mm, millimeter; µm, micrometer; Te, tellurium.

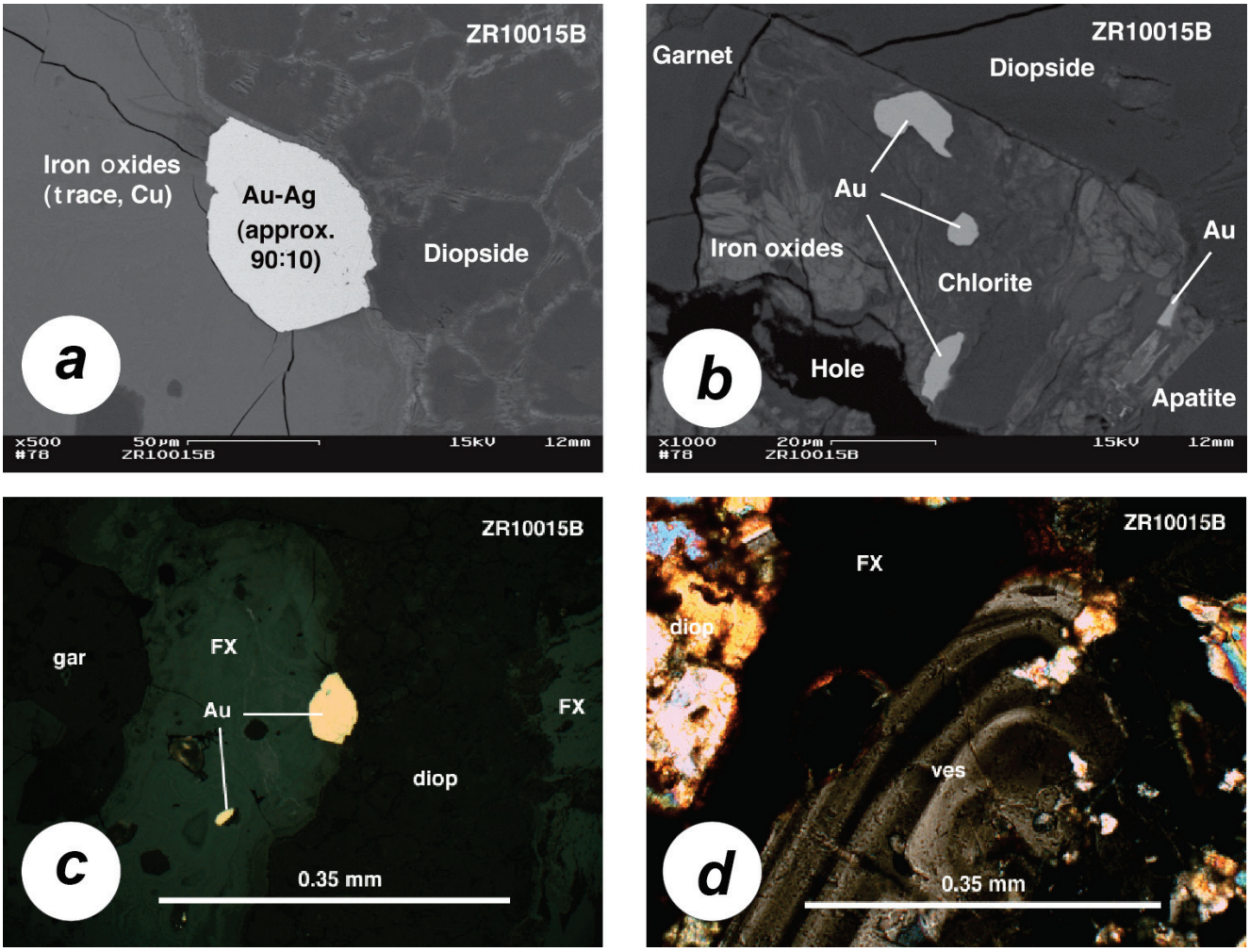

Figure 15A–12. Back scattered scanning electron micrographs of sample ZR10015B showing textural relations within the Zarkashan ores (adapted from Theodore, 2010). (*a*) Gold grain at margin between diopside and iron oxide matte. (*b*) Gold grains within chlorite and iron oxides rimmed by apatite, diopsite, and garnet. (*c*) Gold grain in reflected light shown in (*a*). (*d*) Crystalline vesuvianite also is concentrated adjacent to iron oxide concentrations (from Theodore, 2010). The numbers along the bottom are, from left to right, magnification, scale bar in micrometers, kilovolts used, and working distance, in millimeters (table 15A–2). Ag, silver; Au, gold; Cu, copper; diop, diopsite; FX, iron oxide minerals; gar, garnet; kV, kilovolt; mm, millimeter; µm, micrometer; Te, tellurium; vos, vesuvianite.

The Dynamite and Sufi Kademi prospects lie in the northern parts of the Zarkashan mine area (fig. 15A–14). At Dynamite, a number of north-south trenches have been excavated across an east-trending ridge (fig. 15A–17*a*). Ancient workings are located on the lower parts of the western part of the ridge (figs. 15A–17*b–d*). The Dynamite and Sufi Kademi prospects are summarized by Abdullah and others (1977) from work by Khananov and others (1967) and Meshcheryakov and Borozenets (1970) as described below.

The Dynamite prospect contains zones of shattered ochreous rocks, and a number of 0.6- to 1.2-m-wide zones are present in marmorized limestone of Middle Triassic age along an easterly tending ridge north of the Zarkashan mine subarea (fig. 15A–17*a*). Samples taken for Soviet studies from the walls of ancient openings yielded 4.0 to 70 g/t gold. The iron-stained limestone penetrated by drill holes at depths of 40 to 43 m and 70 to 77 m (presumably under the ancient workings) contains gold concentrations that are less than 0.3 g/t gold (Khananov and others, 1967; Meshcheryakov and Borozenets, 1970).

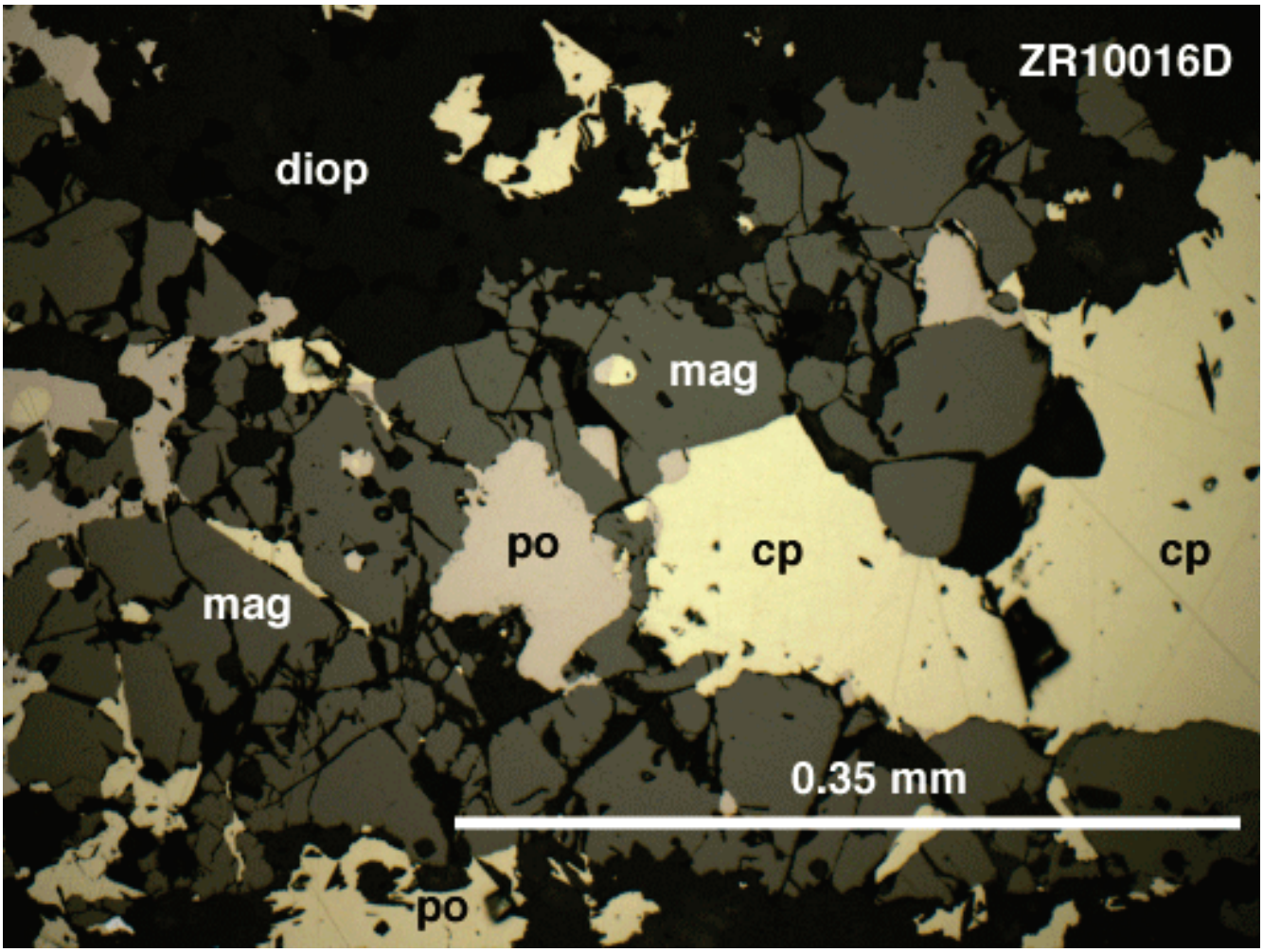

Figure 15A–13. Microphotograph in reflected light of sample ZR10016D (adapted from Theodore, 2010), a diopside- and sparse garnet-marble skarn flooded by sulfide minerals and micas (not indicated) and magnetite. diop, diopside; mag, magnetite; po, pyrrhotite; cp, chalcopyrite (table 15A–2).

Marble and dolomite at the Dynamite prospect are characterized by orange cross-cutting structures, sheeted ochre zones, vuggy ochre and brown patches, and ochre- and bleach-stained altered marble (figs. 15A–18*a–d*). Results of grab samples in the trenches from the mineralized zone yielded less than several parts per billion (ppb) gold, but some samples were anomalous in arsenic [2,560 to 4,870 parts per million (ppm)], manganese (893 to 1,680 ppm), and zinc (trace amounts) (Abdullah and others 1977).

Mineralized zones in the Dynamite area are oxidized, contact metamorphosed, and consist of collapse breccias that include stylolitic solution surfaces. Rocks are made up mostly of calcite and smaller amounts (probably less than 1 vol. %) of 10–µm-wide dolomite crystals (fig. 15A–18). The latter are scattered through calcite. Most rocks contain much less than 1 vol. % iron and manganese oxide, and sulfide minerals are usually not visible with the standard microscope, although 1-µm-wide pyrite grains (probably recrystallized framboids) and 1-µm-wide chalcopyrite grains were detected by SEM (Theodore, 2010). The latter are present in small open cavities together with kaolinite. Some rocks contain signs of incipient recrystallization of pyroxene, probably diopside. These prospected zones at Dynamite may be representative of host rock to mineralized skarn and associated alteration assemblages at Zarkashan.

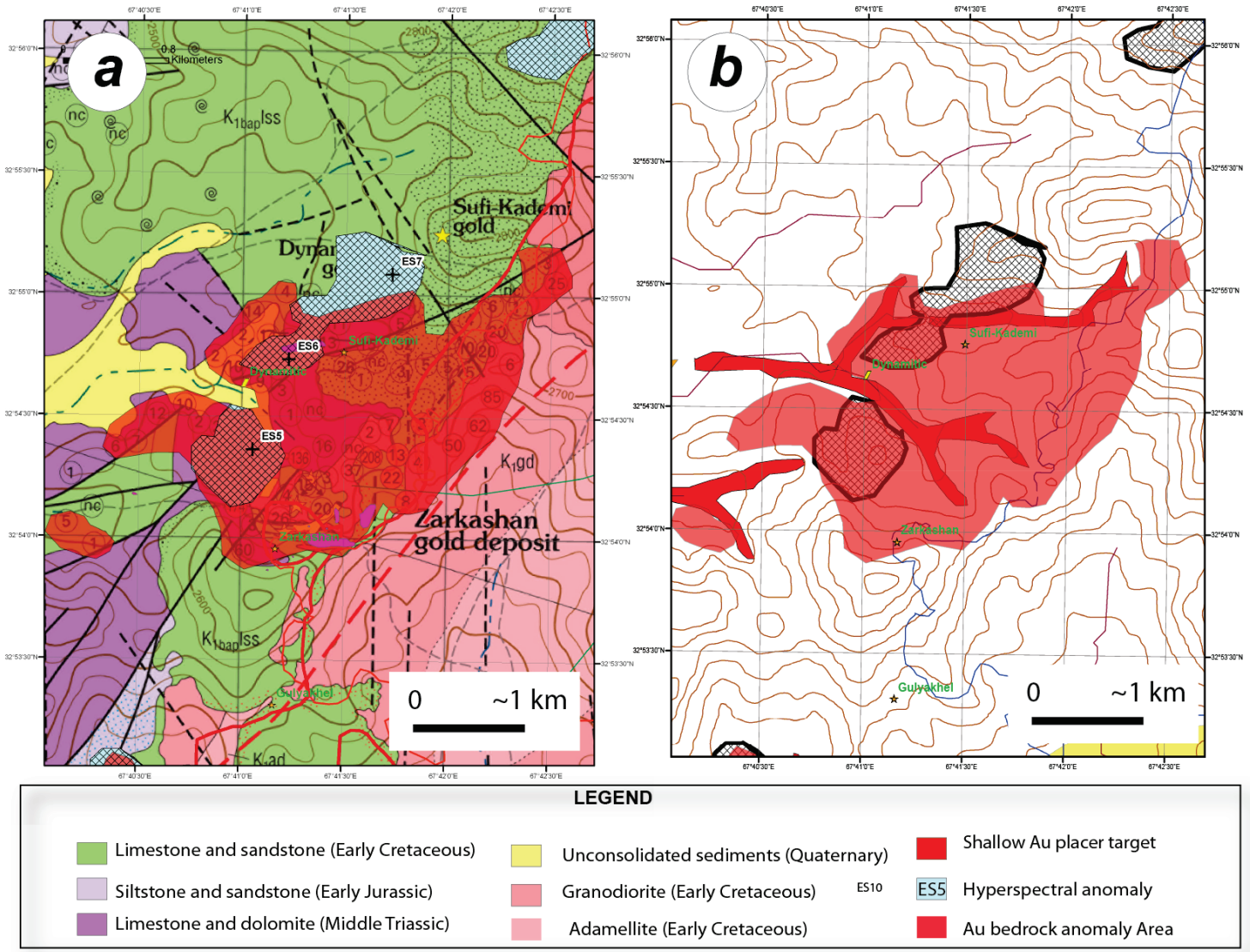

Figure 15A–14. Maps showing the geology and mineralized areas around the Zarkashan mine subarea, including the Dynamite prospect and the Sufi Kadem gold skarn in the northern parts of the target zone. (*a*) Geologic map and gold bedrock anomalies from Peters and others (2011). (*b*) Topographic maps showing anomalous zone and potential zones for shallow gold placer deposits.

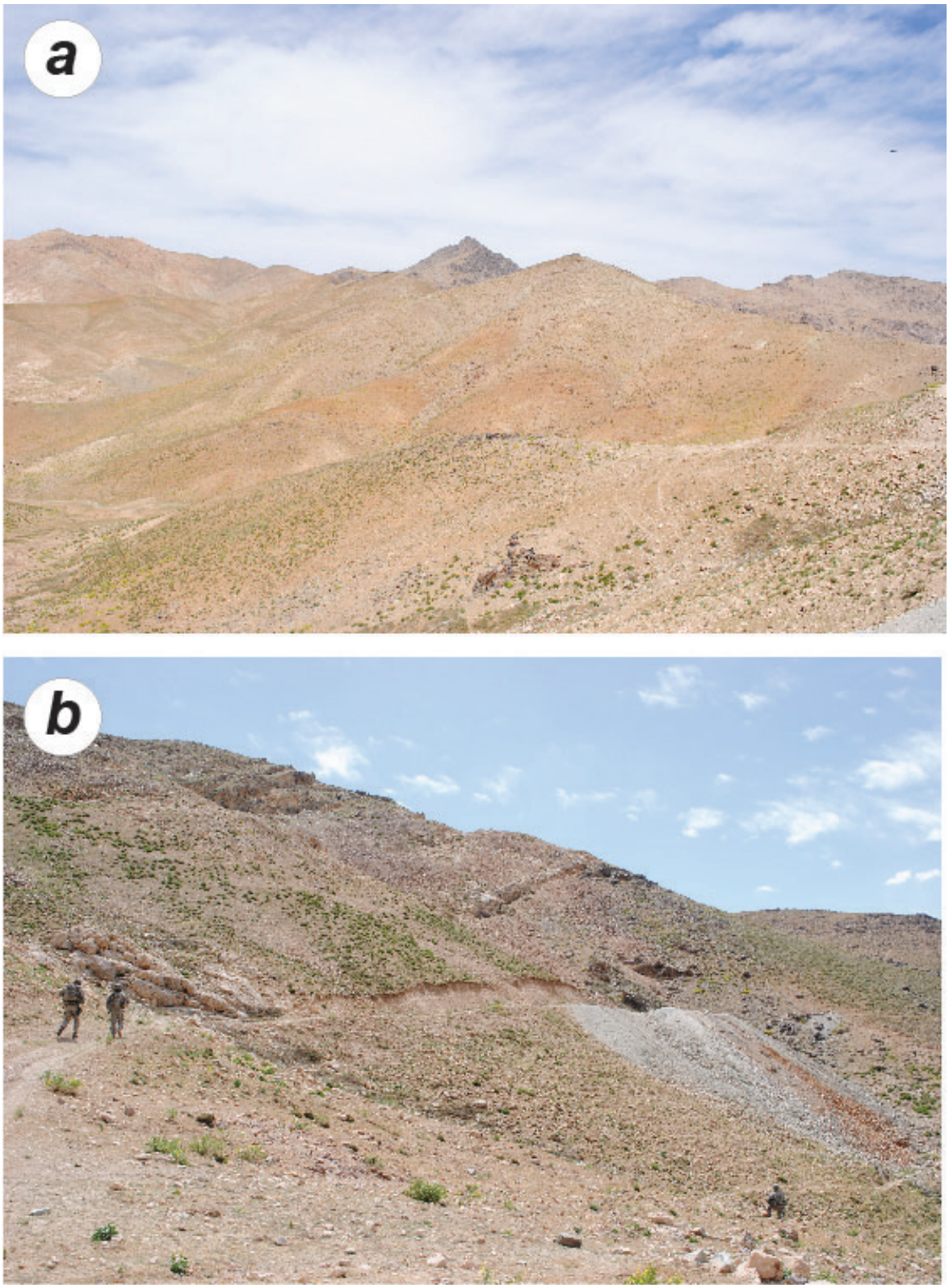

Figure 15A–15. Photographs of the Zarkashan mine subarea. (*a*) View looking west at iron-stained, hornfelsed calcareous mudstone intruded by granodiorite dikes. (*b*) View looking east at trenching and road leading to an eastern sampling adit. Photograph by Stephen G. Peters, U.S. Geological Survey.

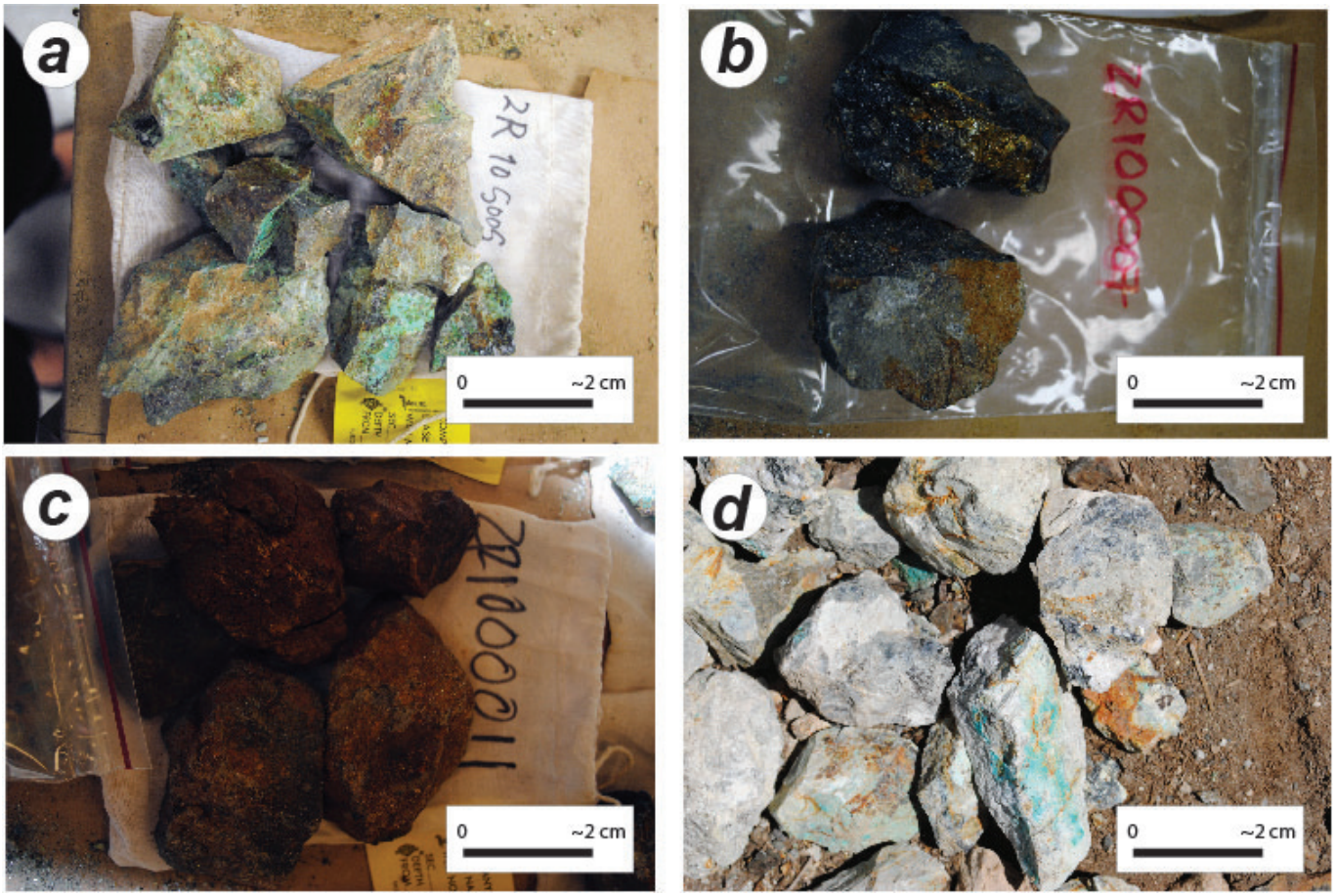

Figure 15A–16. Photographs of typical mineralized rocks from the Zarkashan mine subarea. (a) Malachite-stained hornfelsed mudstone. (b) Sulfide-rich diopside skarn, (c) pyrite-rich, slightly oxidized skarn. (d) Malachite stained calcareous mudstone and marble. Rock samples are listed in table 15A–2. Photographs by Stephen G. Peters, U.S. Geological Survey.

At the Sufi Kademi gold occurrence, irregular gold mineralization is present along a bed of metasomatically altered conglomerate largely made up of limestone pebbles, which is present between Upper Jurassic to Lower Cretaceous hornfelsed rocks. The conglomerate assayed from traces to 7 g/t gold. Samples collected from the walls of an ancient opening assayed 2.5 to 4 g/t gold (Meshcheryakov and Borozenets, 1970).

15A.9 Khinjaktu Target Area

The Khinjaktu target area lies on the eastern side of the Zarkashan pluton in the Zarkashan mine subarea (fig. 15A–6) and occupies a north-northwest-striking zone that penetrates into the pluton from the south (figs. 15A–19 and 15A–20). A gold anomalous zone is defined by Soviet-era sampling (fig. 15A–19). The Khinjaktu prospect contains gold mineralization in skarn at the contact between Upper Jurassic to Lower Cretaceous marmorized limestone and Late Cretaceous to Paleocene diorite (figs. 15A–20*b* and 15A–21*b*). The skarn zone is weathered and is 200 m along strike and rocks from the skarn contain concentrations of 1.8 g/t gold and 0.65 to 1.02 wt. % copper (Meshcheryakov and Borozenets, 1970). Recent grab sampling in the Khinjaktu prospect area from the granite and the contact zone ranged between several to more than 10,000 ppb gold (table 15A–3).

The Zardak gold prospect lies in the Khinjaktu target area on the eastern side of the Zarkashan pluton where mineralization is reported by earlier studies to be confined to a series of faults in Upper Jurassic to Lower Cretaceous limestone that contains brecciated limestone zones and scarce

disseminations of chalcopyrite, pyrite, and occasionally gold. The zones, up to 1 m wide and 50 to 140 m long, and contain 1.2 to 19.4 g/t gold (Meshcheryakov and Borozenets, 1970). Reconnaissance by the USGS and the TFBSO in 2010 in the northern parts of the Zardak prospect suggests that most of the area is covered by limonite and malachite-stained hornfels (fig. 15A–21*a*) intruded locally by igneous breccia bodies (fig. 15A–19 through 15A–21). Grab samples from the area ranged from 14 to 188,000 ppb gold (table 15A–3). Bodies of igneous breccia also contain some gold concentrations up to 27 g/t gold (fig. 15A–22; table 15A–3).

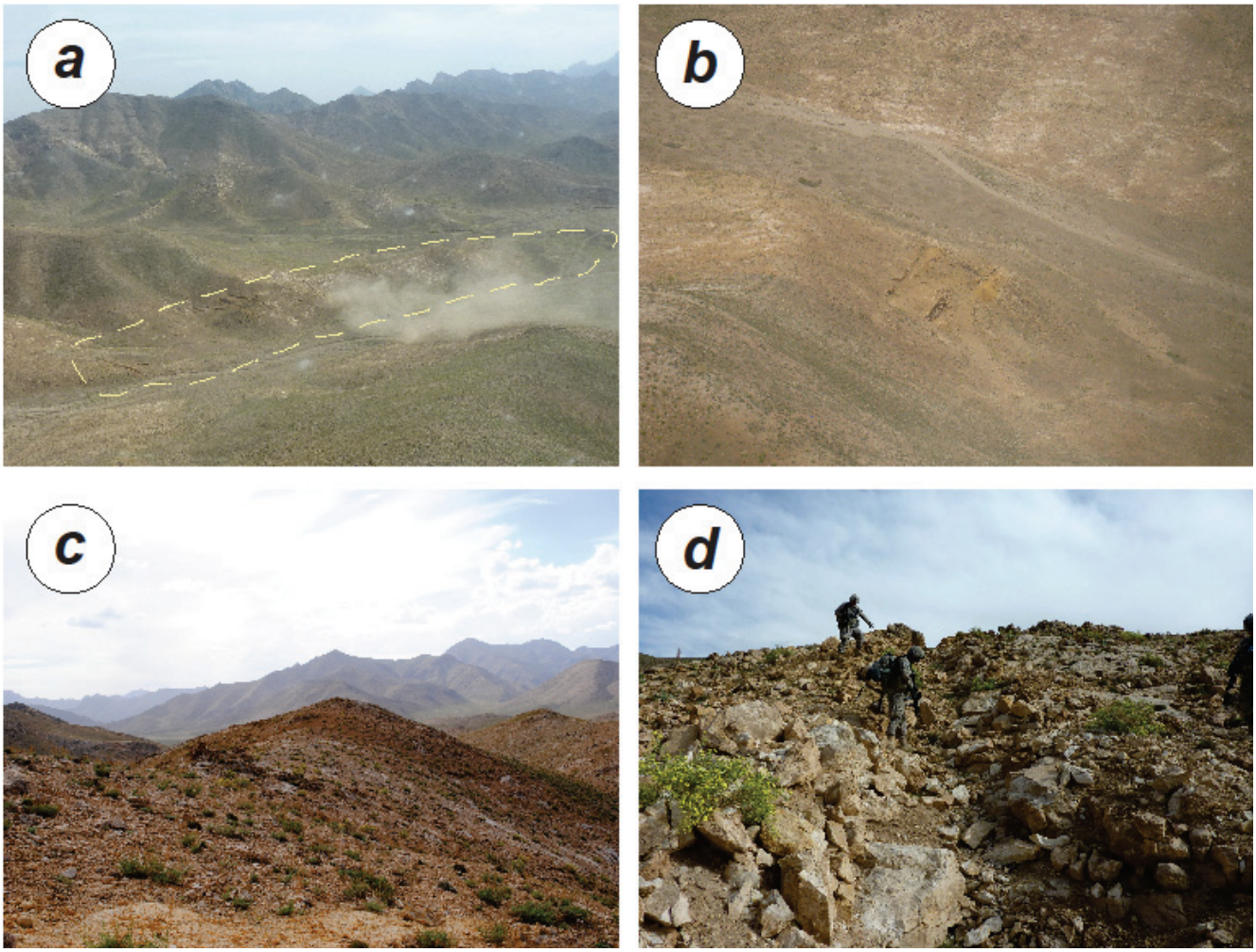

Figure 15A–17. Photographs of the Dynamite prospect area. (*a*) Areal view looking northeast over the Dynamite prospect (outlined with white dashed line). (*b*) Areal view of the eastern part of the Dynamite prospect and possible gold placer drainage to the north. (c) View looking eastwardly in the center of the Dynamite prospect showing ochre alteration. (*d*) View looking northerly in one of many Soviet era trenches. Photographs by Stephen G. Peters, U.S. Geological Survey.

15A.10 Guyakhel Gold Target Area

The Guyakhel gold target area lies within the Zarkashan mine subarea and includes the Guyakhel gold prospect (figs. 15A–6 and 15A–23), which is along a contact between Upper Jurassic to Lower Cretaceous limestone and Late Cretaceous to Paleocene diorite. The contact includes skarn bodies 1 to 1.5 m wide and 50 to 70 m long, containing disseminated bornite, chalcopyrite, covellite, magnetite, and pyrite. Gold concentrations within the mineralized zones are 4.4 g/t gold (Khananov and others, 1967). A number of gold anomalous zones are indicated by pan concentrate(?) sampling in the drainages south of the Guyakhel gold prospect in the southern sedimentary rocks (fig. 15A–23).

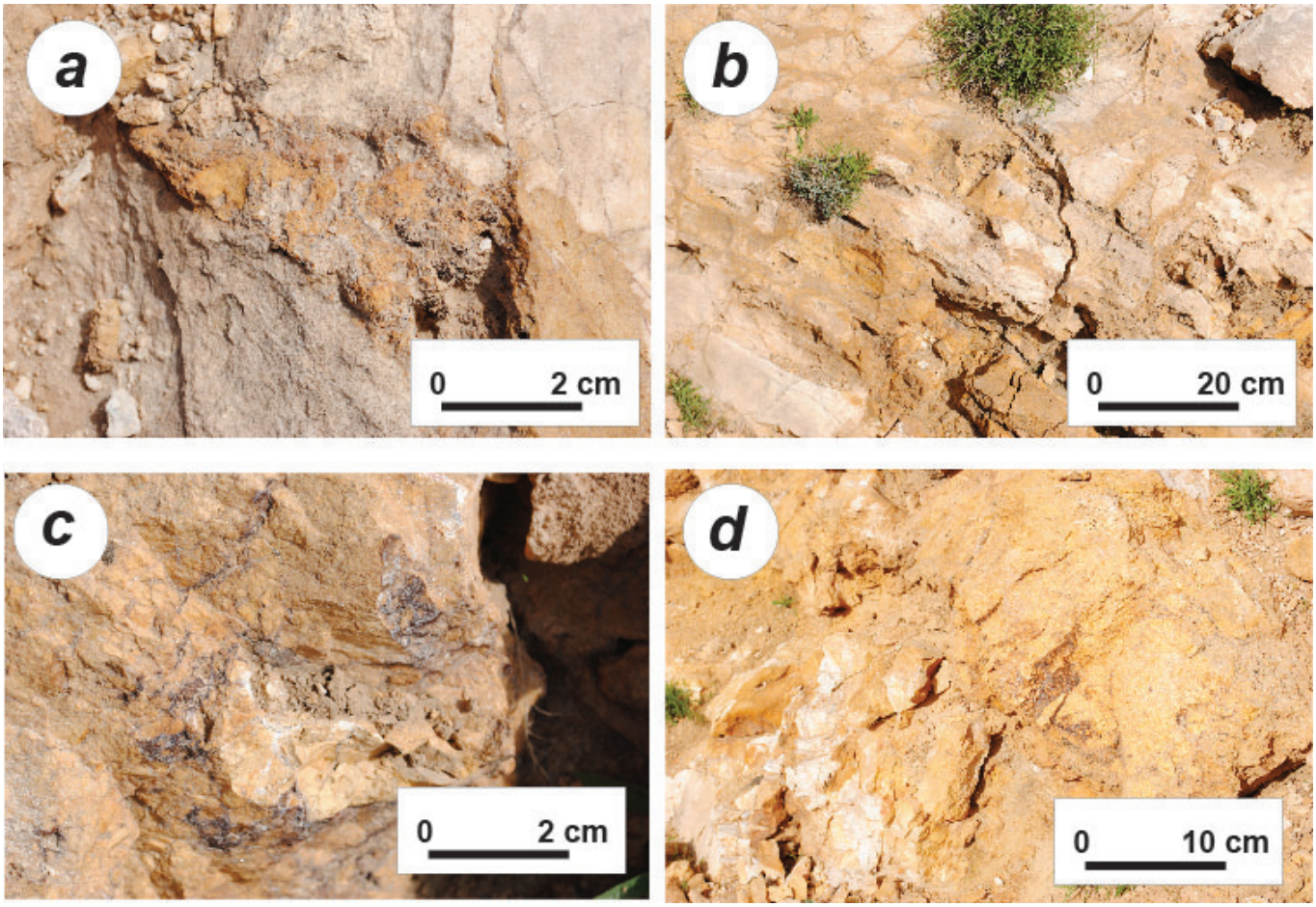

Figure 15A–18. Photographs of marble and dolomite from trenches in the Dynamite prospect area. (*a*) Orange cross cutting zone. (*b*) Sheeting of ochre zones across marble. (c) Vuggy ochre and brown areas in dolomite-marble. (*d*) Ochre staining and bleaching of altered marble. cm, centimeter. Photographs by Stephen G. Peters, U.S. Geological Survey.

Table 15A–3. Gold concentrations of samples taken at the Zardak-Khinjaktu target area in 2010.
[Latitude and longitude are in decimal degrees. Au, gold; ppb, parts per billion; >, more than]

Sample no.	Latitude	Longitude	Description	Prospect	Au, in ppb
ZA100001	32.89676	67.74141	malachite stained spotted hornfels	North Zardak	17,000
ZA100002	32.89676	67.74141	argillically altered diorite breccia	North Zardak	14
ZA100003	32.89676	67.74141	argillically-altered igneous breccia	North Zardak	14
ZA100004	32.89676	67.74141	malachite-stained argillically-altered diorite breccia	North Zardak	27,000
ZA100005	32.89676	67.74141	marble grey	North Zardak	82
ZA100006	32.89676	67.74141	malachite-stained hornfels	North Zardak	188,000
ZA100006	32.89780	67.73945	malachite-stained hornfels	North Zardak	17,000
ZA105001	32.90510	67.73550	limonite-stained marble	Khinjaktu	1,190
ZA105002	32.90510	67.73550	limonite-stained marble	Khinjaktu	27
ZA105003	32.90510	67.73550	limonite-stained marble	Khinjaktu	17
ZA105004	32.90510	32.90510	limonite-stained diorite	Khinjaktu	45
ZA105005	32.90510	67.73550	malachite-stained gossan-hornfels	Khinjaktu	>10,000

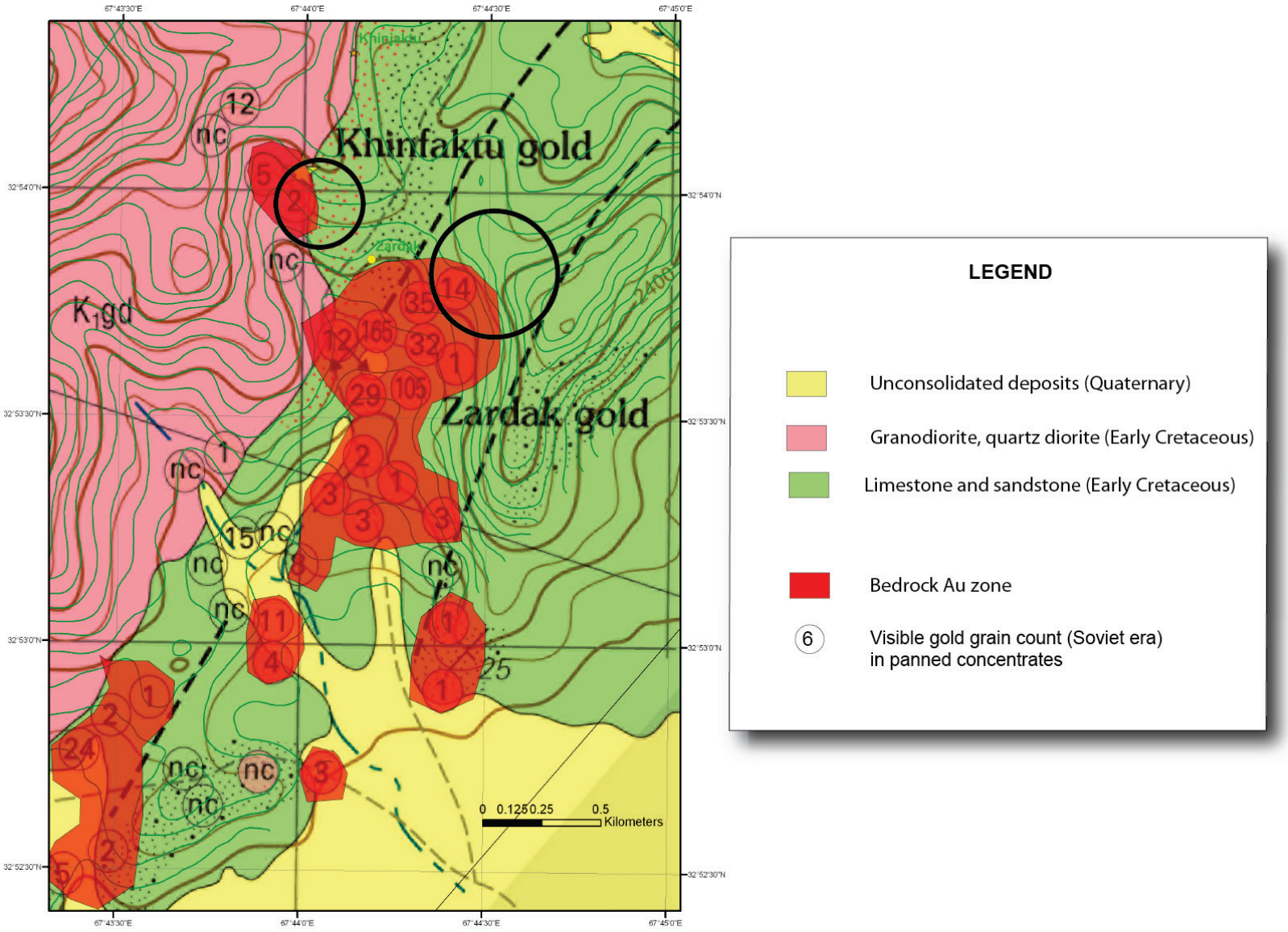

Figure 15A–19. Geologic map and targets of the Zardak-Khinjaktu target area, showing hardrock gold zones sampled during Soviet-era studies (reproduced in Peters and others, 2011). Areas sampled in 2010 and listed in table 15A–3 are in open black outlined circles. Au, gold.

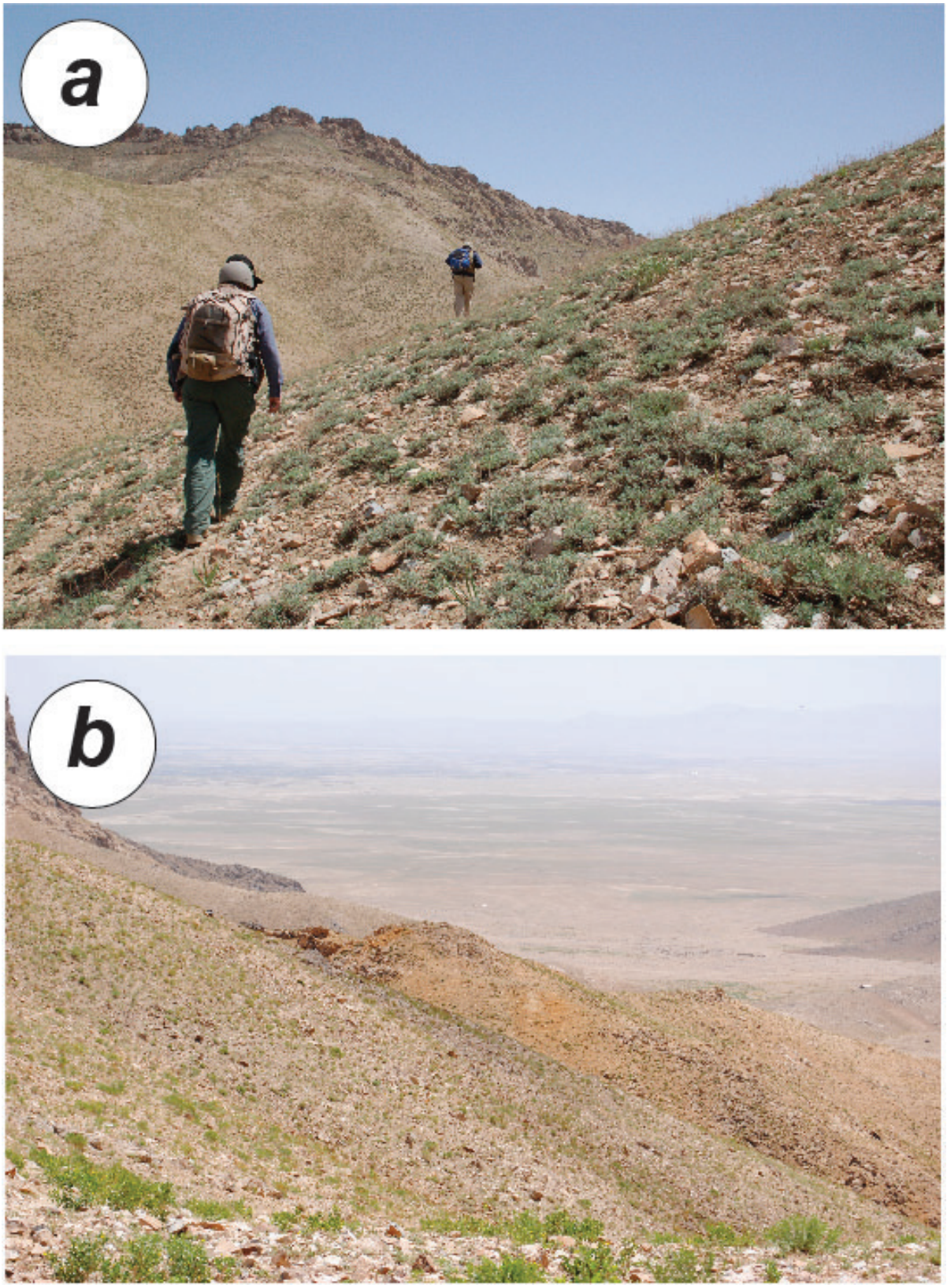

Figure 15A–20. Photographs of landscape and area around the Zardak-Khinjaktu target area. (*a*) View looking west with hornfels in foreground and Zardak intrusive in jagged outcrops on the skyline. (*b*) View looking south southeast toward Khinjaktu skarn workings (orange outcrops). Photographs by Stephen G. Peters, U.S. Geological Survey.

Figure 15A–21. Photographs of specimens taken from the Zardak-Khinjaktu area in 2010. (*a*) Sample ZAR105005, oxidized, malachite-bearing skarn from the Khinjaktu prospect. (*b*) Sample ZA 100006, malachite-stained hornfelsed mudstone from above the Zardak prospect area. Samples are listed in table 15A–3. Photographs by Stephen G. Peters, U.S. Geological Survey.

Figure 15A–22. Photograph of igneous breccia float in the old Zardak prospect area. The boulders are isolated within the hornfels zone and may constitute a breccia dike or pipe. cm, centimeter. Parts of this breccia contain as much as 27,000 g/t gold (table 15A-3). Photograph by Stephen G. Peters, U.S. Geological Survey.

15A.11 Bolo Gold Subarea

A number of gold prospects are present along a northeast-trending linear zone in the western part of the Zarkashan copper and gold AOI in the Bolo gold subarea (figs. 15A–4 and 15A–24).

The Alaghzar gold prospect is present in a fault zone in Upper Permian marble and in Devonian quartzitic sandstone and conglomerate that are intruded by Late Cretaceous to Paleocene diorite. At the exocontacts of the diorite bosses, the mineralized zones are skarn lenses that are from 0.1 to 11 m thick and as much as 100 m long. The 70- to100-m-wide and 500-m-long mineralized zones also contain serpentinized and limonitized rocks containing sulfide minerals. The skarns assay from 0.01 to 1.6 g/t gold (Douvgal and others, 1971). The serpentized zones contain chalcopyrite and hematite, with concentrations of as much as 35 g/t gold and 0.1 to 3.1 wt. % copper. The limonitized limestone assays not more than 0.2 g/t gold and is present in patches that enclose streaks of serpentine. The presence of chalcopyrite may increase the gold content to 35 g/t gold (Douvgal and others, 1971).

The Anguray gold prospect (fig. 15A–24) is in a mineralized zone that is along a contact between Upper Permian carbonate rocks and Late Cretaceous to Paleocene quartz-diorite. The zone consists of garnet skarn and pyroxene and is as much as 1 m thick and several tens of meters long. The mineralization consists of scarce disseminations of bornite, chalcopyrite, and covellite. Gold content varies from 0.3 to 143 g/t gold. In addition, the rocks carry as much as 0.6 wt. % copper, as much as 3.7 wt. % lead, and as much as 2.6 wt. % zinc (Khananov and others, 1967).

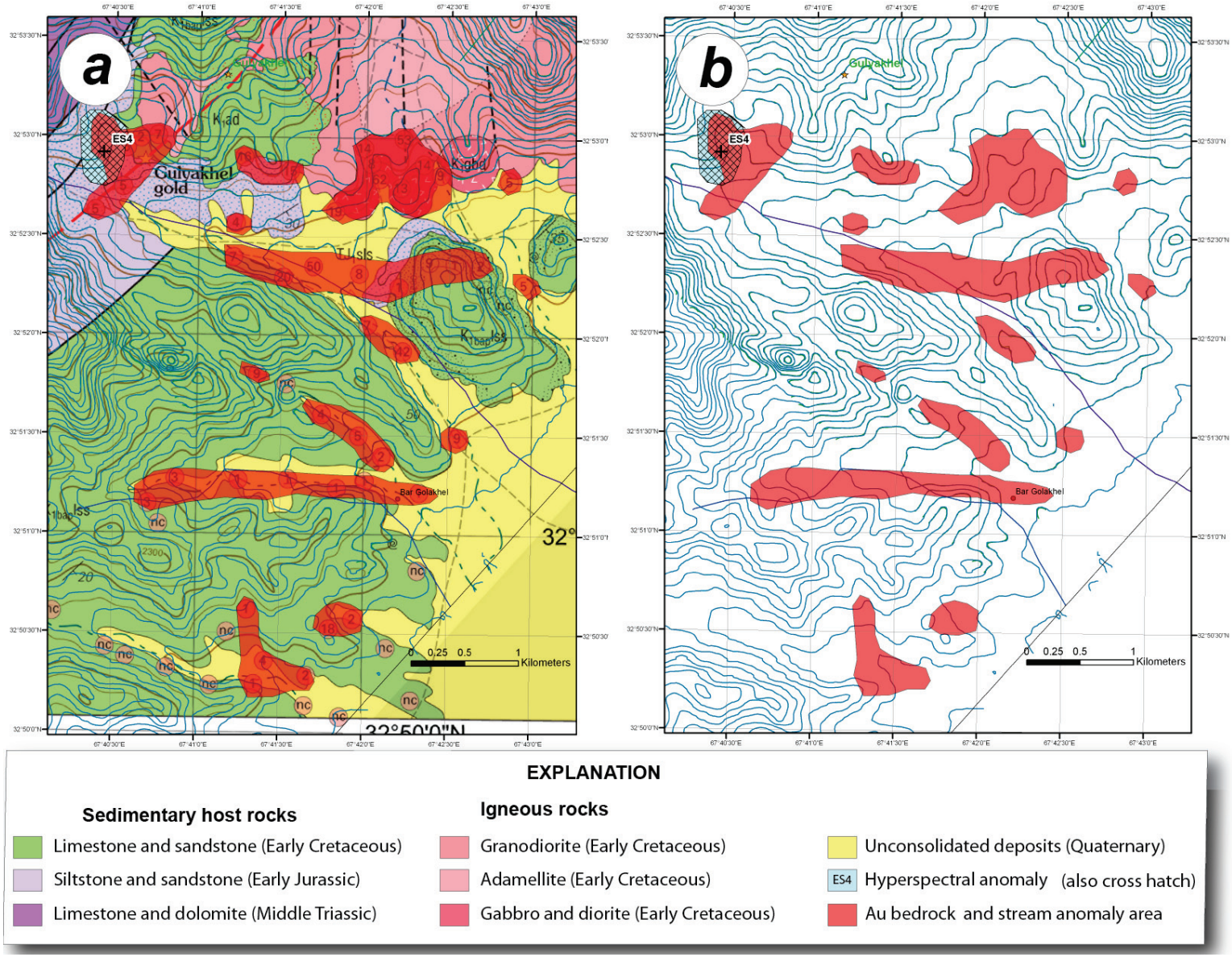

Figure 15A–23. Maps of the Guyakhel target area. (*a*) Geology from Peters and others (2011), showing bedrock gold anomalous zones (samples and grain counts are circles, nc = no count). (*b*) Topographic map showing gold anomalous zones.

The Bala gold prospect (fig. 15A–24) consists of mineralized rock along a fault zone in upper Permian limestone where the rock is intensely brecciated and ochreous. The zone, 0.5 to 12 m wide and 140 m long, assays between 0.8 and 34 g/t gold (Douvgal and others, 1971).

The Bashargar occurrence is at the contact between Upper Triassic marmorized carbonate rocks and Late Cretaceous to Paleocene diorite stocks. There are four lenses of diopside-vesuvianite skarn 1 m in thickness and 50 to 80 m in extension. Gold content is from 2.9 to 12.3 g/t gold. A higher content reaching 43 g/t gold has been reported from the limonitized limestone (Khananov and others, 1967).

The Belaw gold occurrence is confined to a contact between Late Cretaceous to Paleocene diorite bodies and Upper Permian marble (fig. 15A–24 through 15A–26). Gold is present in skarn (1 m × 10 m in size) and in 2- to 25-m-wide and as much as 250-m-long zones of ochreous and serpentinized rocks. Ore minerals are chalcopyrite, native gold, and pyrite. The skarn and serpentinized rocks assay from 0.1 to 0.8 g/t gold and 0.1 wt. % copper. The ochreous zones carry from 1 to 4 g/t gold, 0.3 wt. % copper, and 0.5 wt. % zinc (Douvgal and others, 1971).

The Utkul gold prospect contains gold mineralization that is localized in a fault zone in Late Permian marmorized and dolomitized limestone (fig. 15A–24). The zone is 300 m long and 0.5 m wide. Gold is associated with sulfide minerals in slightly ochreous rocks forming patches, 1 to 5 m by 5 m in size. The highest gold content is 11 g/t Au (Khananov and others, 1967).

15A.12 Luman-Tamaki Gold Subarea

The Luman-Tamaki gold subarea is located within a northeast-striking tectonic zone containing Middle Paleozoic sedimentary rocks encompassing polymetallic vein and copper skarn mineral occurrences (fig. 15A–28; Peters and others, 2007). The mineralized tectonic zone lies between the Arghandab batholithic rocks to the northwest and other sedimentary rocks to the east. The Luman-Tamaki gold subarea contains phyllic and argillic altered areas recognized by ASTER (Mars and Rowan, 2007), parallels a northeast-striking fault along the southeast margin of the mineralized zone, and includes a prospective zone that is approximately 20 to 25 km long and 2 km wide.

A number of occurrences in this prospective Tamaki-Luman gold subarea are gold-rich, such as the Tamaki gold occurrence that is 600 m long and 2 to 15 m wide and contains chalcopyrite and galena in irregular siliceous lenses and grades 0.1 to 50.0 g/t gold with traces of lead and zinc (Abdullah and others, 1977; Borozenets, 1972). The Luman gold occurrence is as much as 60 m long and 0.5 to 1.5 m wide and grades 1.4 g/t gold and 1.0 wt. % copper (Douvgal and others, 1971). In addition, a number of unnamed precious- and basemetal-vein and skarn occurrences are present within the Luman-Tamaki gold subarea. The main data for the Tamaki-Luman gold subarea are aeromagnetic and geologic maps, lithogeochemical data, mineral deposits database, and ASTER imagery (Orris and Bliss, 2002; Doebrich and others, 2006; Sweeney and others, 2006; Mars and Rowan, 2007).

Ludington and others (2007) and Peters and others (2007) noted the information most needed in the Luman-Tamaki gold subarea is intermediate-scale (1:100,000 and 1:25,000) geologic mapping, geochemical sampling, and detailed examination of known prospects. All these approaches would require extensive site visits. The presence of widespread prospects of pluton-related and base- and precious-metal occurrences is a positive indicator that commercial mineralized zones may be present. The presence of widespread phyllic and argillic alteration in ASTER imagery (fig. 15A–29) is also a positive indicator; however, many alteration patterns appear to be related to regional fractures within the batholith, and most do not correlate well spatially with distribution of mineral prospects. The composition of Arghandab batholithic rocks is not highly favorable; there are many peraluminous rocks exposed and a dearth of intermediate and mafic rocks (diorite), both somewhat atypical of porphyry-bearing terranes. The Luman-Tamaki gold subarea lies along strike of the Bolo gold subarea and may also contain Zarkashan igneous rocks along its linear structures.

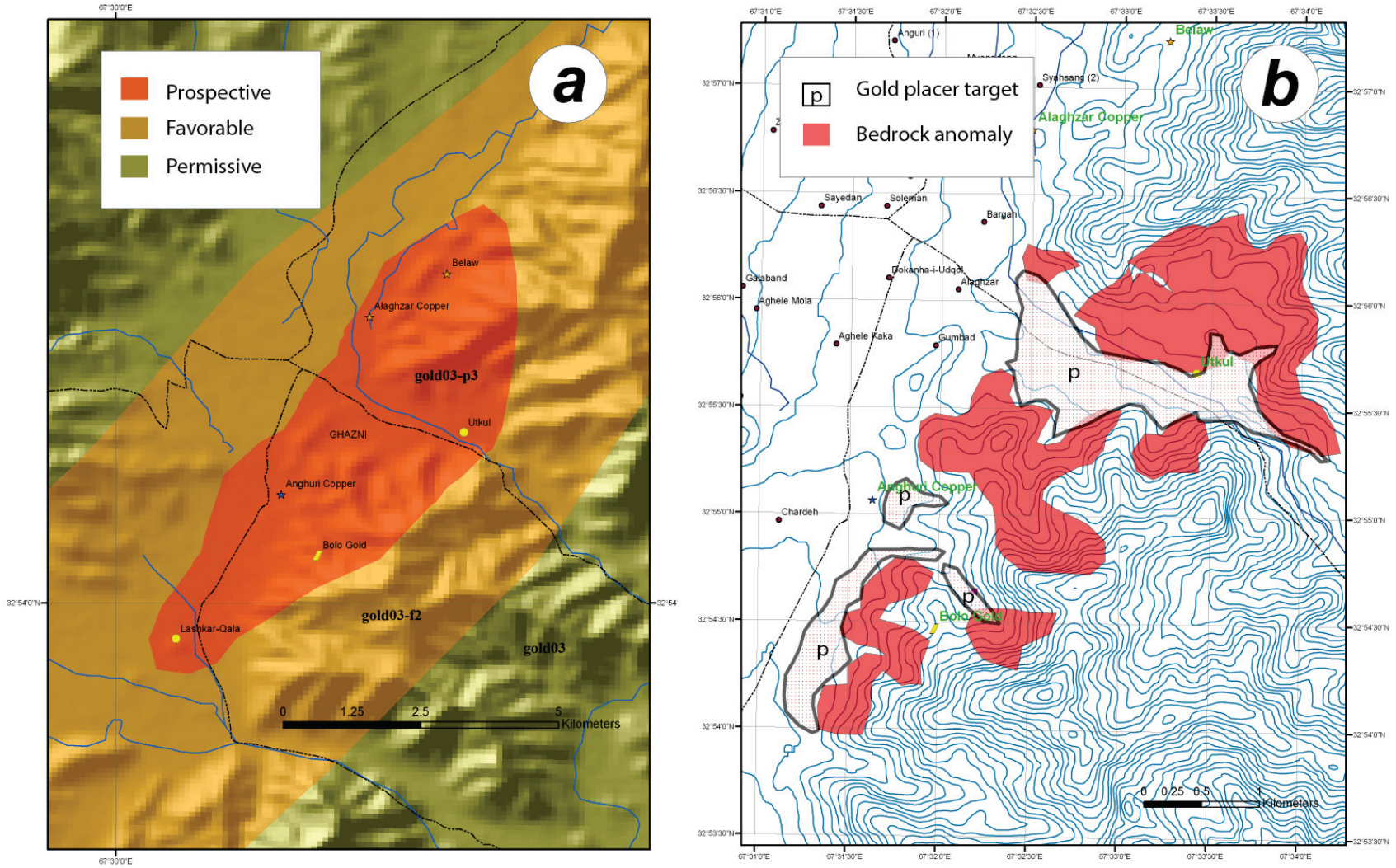

Figure 15A–24. Maps of the Bolo gold subarea showing mineralized areas. (*a*) Permissive, favorable, and prospective tracts from Peters and others (2007) (*b*) Bedrock anomalies from grain counts from Soviet era studies, reproduced in Peters and others (2011), and potential shallow gold placer targets.

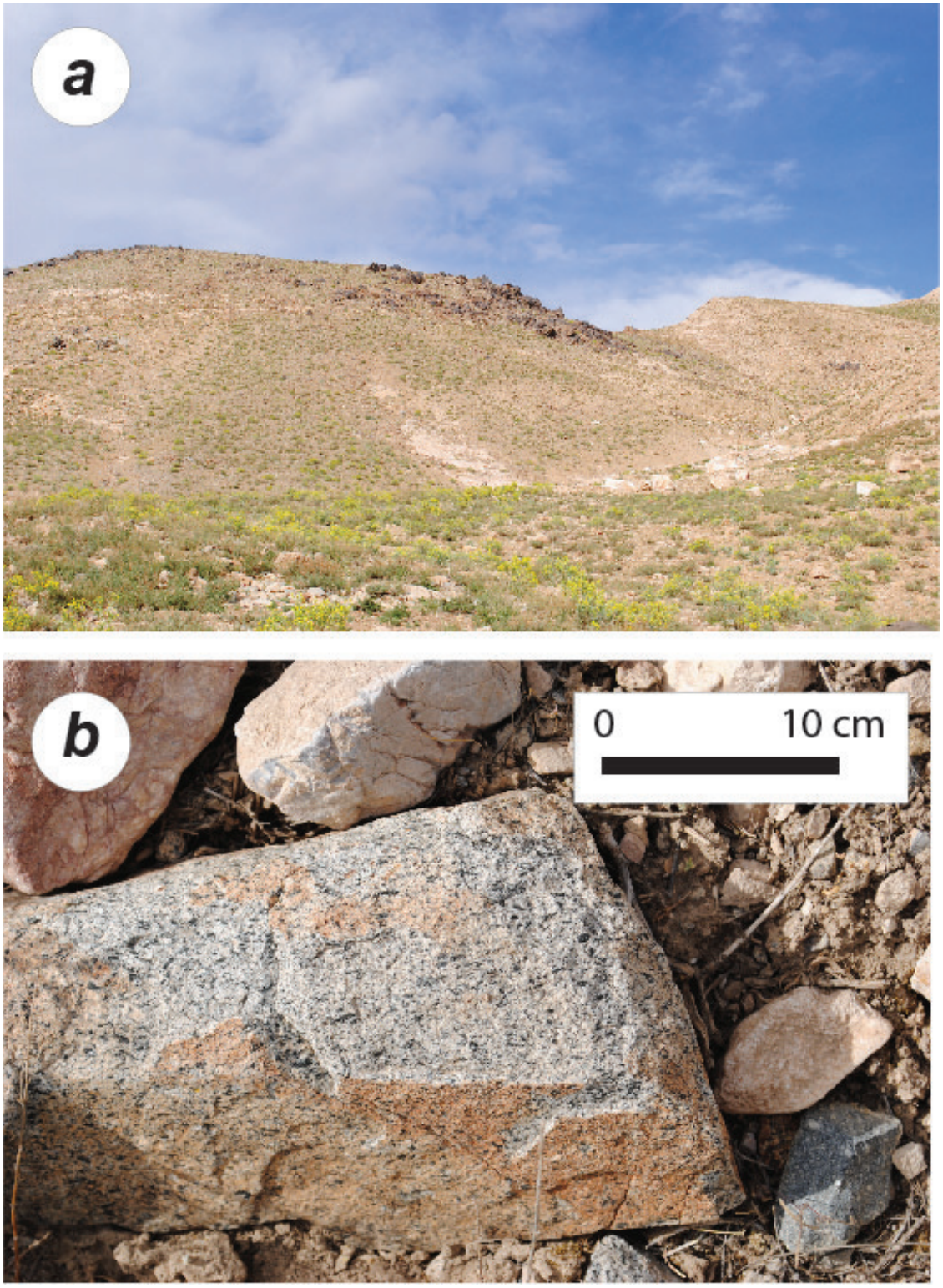

Figure 15A–25. Photographs from the Bolo gold prospect. (*a*) View to the south showing ochre alteration in limey rocks and shallow prospects on hillside. (*b*) Hornblende "diorite" cobble in Bolo gold streambed. cm, centimeter. Photograph by Stephen G. Peters, U.S. Geological Survey.

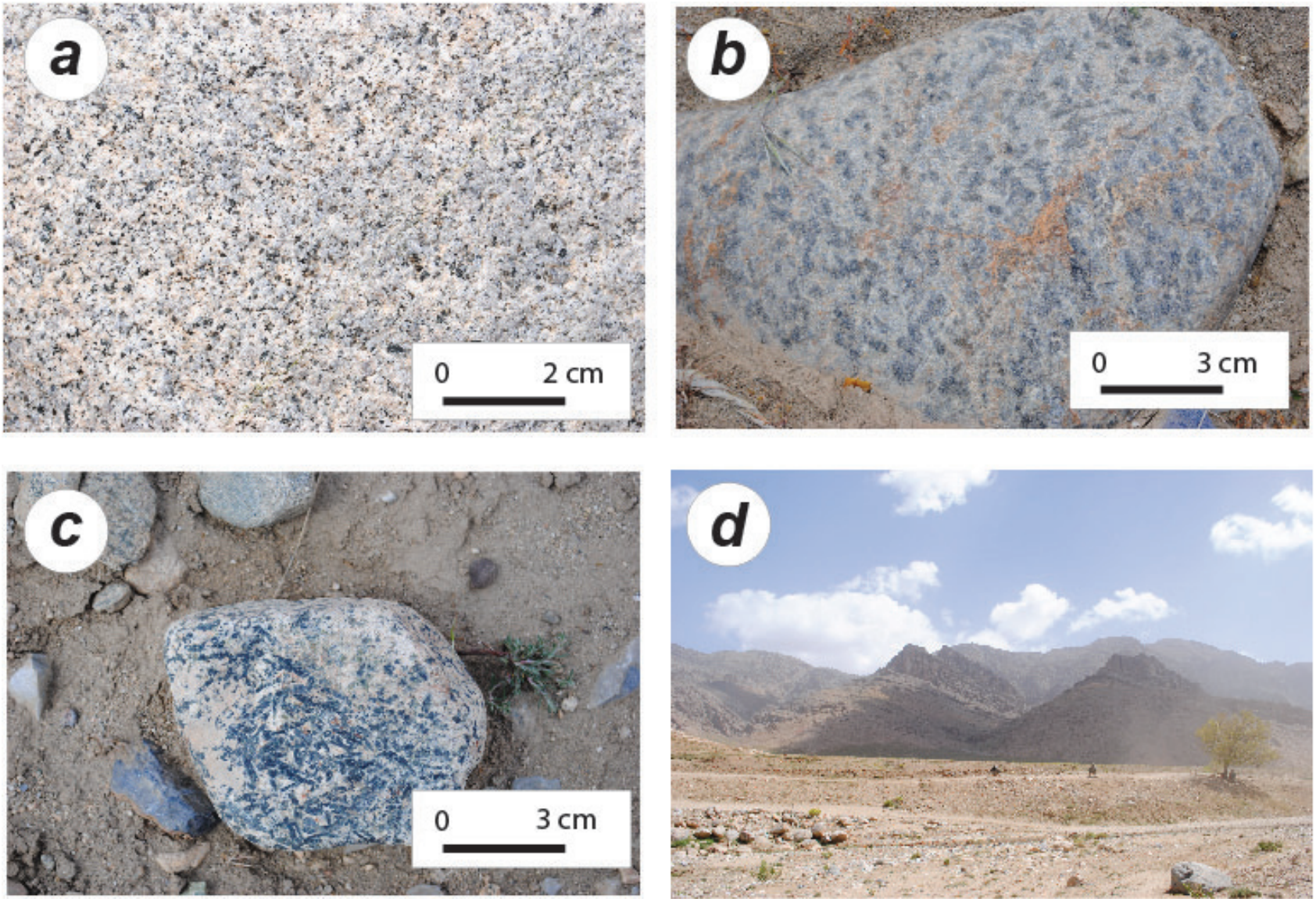

Figure 15A–26. Photographs from the Utkul gold prospect area in the Bolo gold subarea. (*a*) Diorite stream boulder. (*b*) Porphyroblastic contact metamorphic rock, stream cobble. (*c*) Bladed porphyroblastic contact metamorphic rocks, stream float. (*d*) View to northeast looking at anomalous zones in hills composed of Middle Triassic limey rocks. cm, centimeter. Photographs by Stephen G. Peters, U.S. Geological Survey.

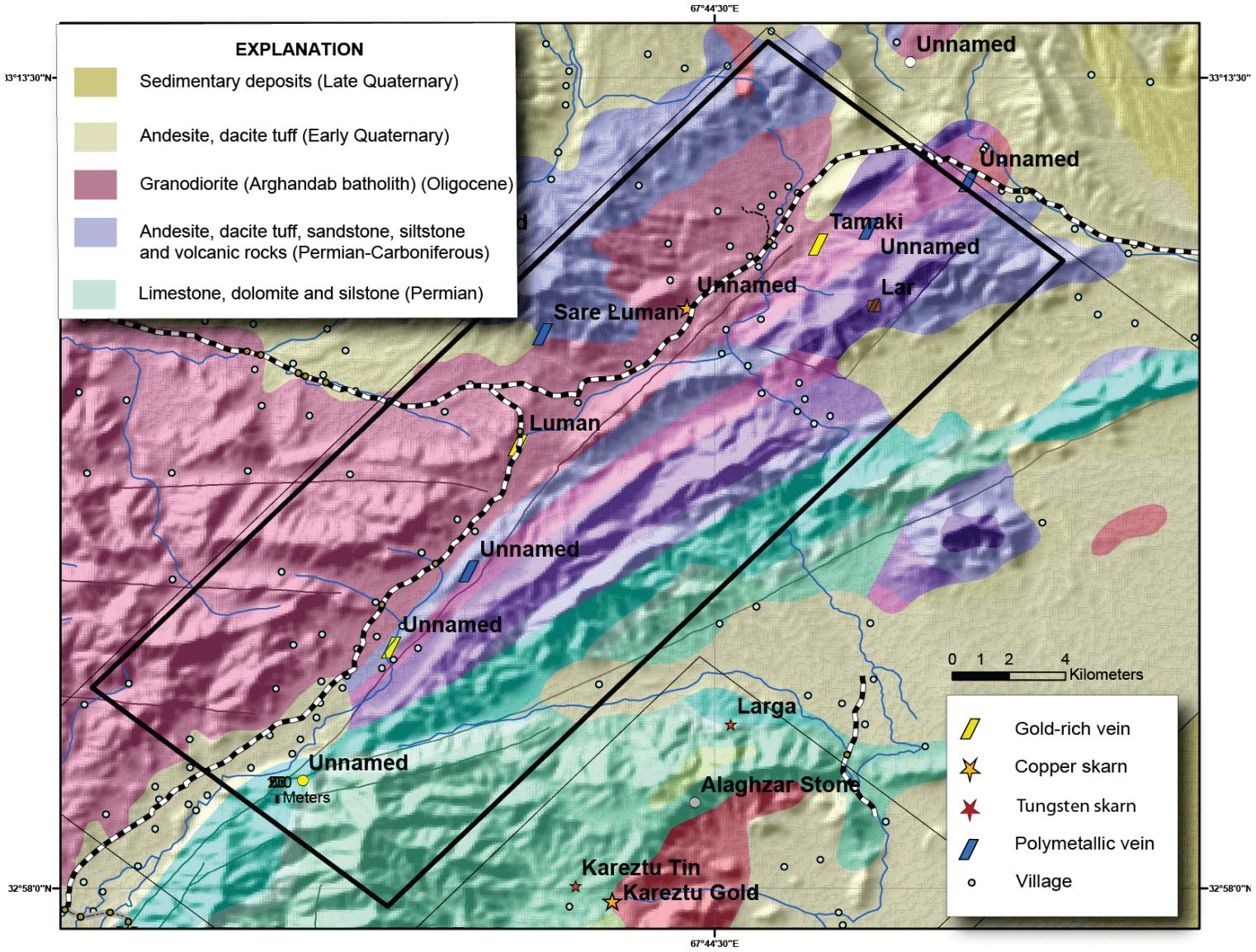

Figure 15A–28 Map showing geology and gold-rich mineral occurrences in the Luman-Tamaki gold subarea. The northeast-trending linear valley may represent a significant regional-scale fault zone. Geology from Doebrich and others (2006).

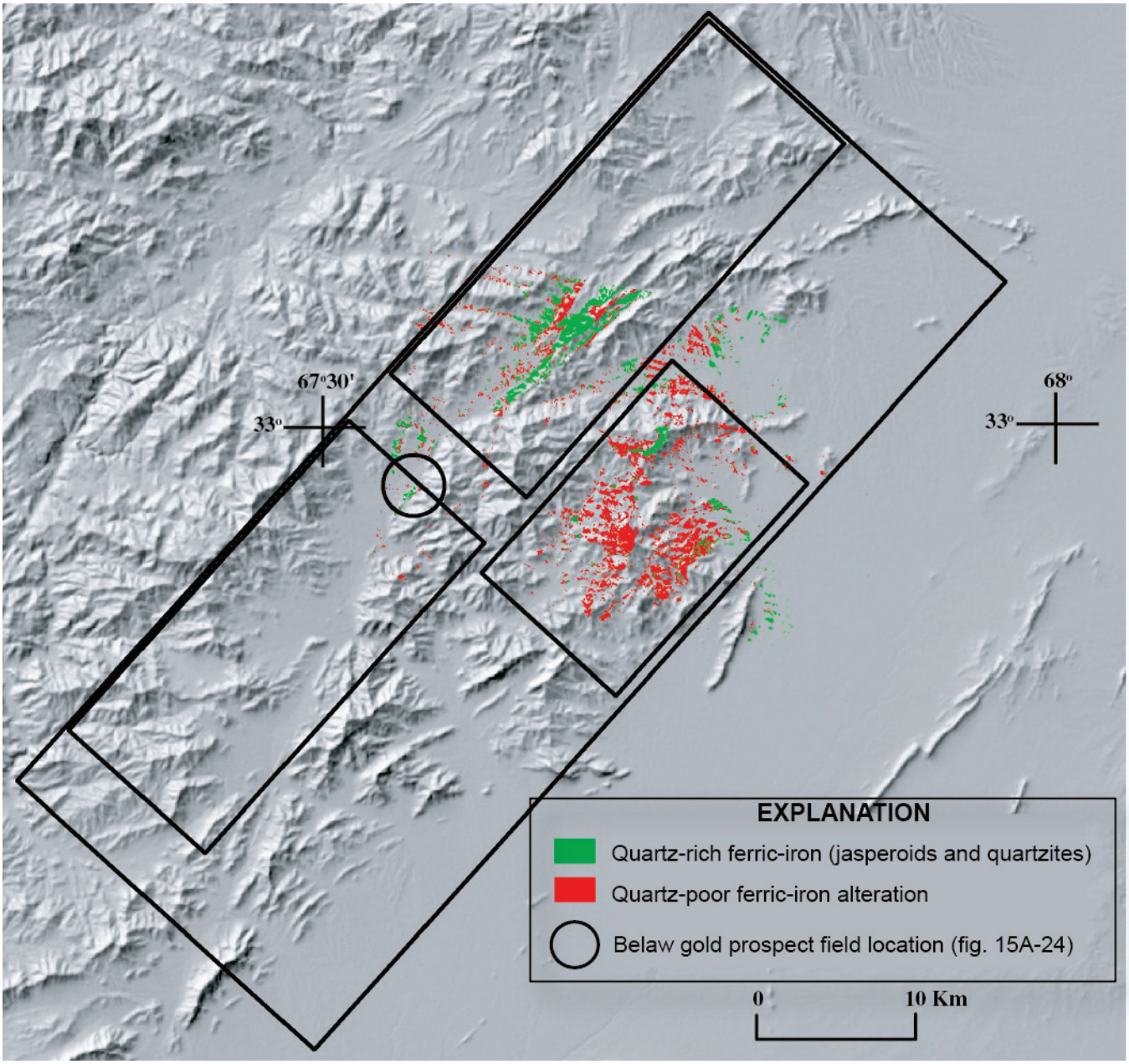

Figure 15A–29. Digital elevation map showing Advanced Spaceborne Thermal Emission and Reflection radiometer -derived ferric-iron and silicic (quartz) alteration patterns for most of the Zarkashan mine subarea, half of the Luman-Tamaki gold subarea, and a small (topmost) part of the Bolo gold subarea validated in the field (circled area).

15A.13 Placer Gold Potential

There are three main types of gold placer targets in the Zarkashan copper and gold AOI—shallow, intermediate, and deep. The shallow gold placer targets are those that are less than 3 m deep and are in small drainages around known bedrock anomalous zones (fig. 15A–30). The shallow gold placer targets can be worked by artisans and local labor by hand with minimal equipment. The intermediate targets are those that may be greater than 3 m deep and less than 10 m deep and could be worked by small mechanized means, either a bulldozer or a back hoe, in combination with the use of a sluice box. The deep gold placer targets are those that were identified in the USGS preliminary assessment (Peters and others, 2007), may be deeper than 10 m and as much as 30 m deep, and could be

worked by water dredge or other large, capital-intensive excavation methods. These deeper deposits would be explored with drilling and could extend into the main valleys to the southeast and east of the Zarkashan copper and gold AOI (fig. 15A–30).

A 3- to 6-km-long Zarkashan gold shallow to intermediate depth placer deposit is known within the Zarkashan copper and gold AOI. Evaluations have taken place for gold placer deposits in the Zarkashan copper and gold AOI, leading to some resource calculations (Homilius, 1968, 1970). The known shallow Zarkashan gold placer deposits are in the northern part of the Zarkashan mine subarea and in a 3–km-long and 200–m-wide valley that contains 1.2- to 2.5-m-thick gold-bearing sedimentary layers near the bedrock. The overburden is 1.5 to 11 m deep. Resources calculated over the main part of the gold placer are 116 kilograms of gold, averaging 1,111 milligrams per cubic meter (mg/m^3) gold. The gold-bearing sedimentary pay streak is 104,400 cubic meters (m^3) in size with an average 2-m thickness (Homilius, 1968, 1970; Meshcheryakov and Borozenets, 1970; Abdullah and others, 1977).

A permissive tract for deep gold placer deposits was constructed by Peters and others (2007) in the 180-km-long valley and stream and fan sediments below the two hard rock favorable areas for pluton-related gold adjacent to and within parts of the Zarkashan copper and gold AOI (fig. 10.5A–30) in map units Q_{34}ac, Q_{31}oe, and Q_3c (Doebrich and others, 2006). In addition, upstream active placer areas were also designated as part of the tract.

15A.14 Summary of Hard Rock Potential

The Zarkashan copper and gold AOI has potential for porphyry copper-gold and related and associated mineral deposits. Porphyry copper and copper-gold deposits are large, relatively low-grade deposits that may also contain significant amounts of molybdenum and gold as byproducts. These deposits generally require between hundreds of millions and (or) billions of dollars in capital investment in the construction phase and also require a significant power and transportation infrastructure. Development from the time of discovery to first production may take up to 10 years or more. The porphyry deposits commonly are mined in large open pit mines, but especially rich deposits may also be mined by underground methods. Porphyry copper and copper-gold deposits are commonly spatially associated with a number of high-grade deposit types, such as skarns and polymetallic veins, that are genetically related to a common hydrothermal system. These small but high-grade satellite deposits, such as those in the Zarkashan copper and gold AOI, commonly serve as exploration guides to the larger deposits, and study of the small deposits may lead to discovery of central porphyry copper systems. A summary and references to the appropriate occurrence and grade and tonnage models for all these deposit types are given in table 15A–4.

Table 15A–4. Median tonnage and grade for porphyry copper and copper-gold and associated deposit models.
[Median tonnage and grade data refer to models in Cox and Singer (1986). Ag, silver; Au, gold; Cu, copper; Fe, iron; g/t, grams per metric ton; Mo, molybdenum; Mt, million metric tons; nd, no data; Pb, lead; wt. %, weight percent; Zn, zinc]

Model	Median tonnage, in Mt	Median grade[1]	References
Porphyry copper	220	0.44 Cu, 0.01 Mo, 1.2 Ag, 0.077 Au	Cox, 1986c; Singer and others, 2008.
Porphyry copper-gold	220	0.44 Cu, 0.002 Mo, 1.4 Ag, 0.4 Au	Cox, 1986e; Singer and others, 2008.
Porphyry copper-molybdenum	270	0.45 Cu, 0.028 Mo, 1.5 Ag, 0.012 Au	Cox, 1986d; Singer and others, 2008.
Porphyry copper, skarn-related	80	0.98 Cu, 1 Ag	Cox, 1986d; Singer, 1986.
Cu skarn	0.56	1.7 Cu	Cox and Theodore, 1986.
Zn-Pb skarn	1.4	5.9 Zn, 2.8 Pb, 0.09 Cu, 58 Ag	Cox, 1986e; Mosier, 1986.
Fe skarn	7.2	50 Fe	Cox, 1986a; Mosier and Menzie, 1986.
Polymetallic veins	nd	nd	Cox, 1986b.
Polymetallic replacement	1.8	5.2 Pb, 3.9 Zn, 0.094 Cu, 150 Ag, 0.19 Au	Morris, 1986; Mosier and others, 1986a.

[1]Median grades are in weight percent for copper, molybdenum, lead, and zinc and in grams per metric ton for gold and silver.

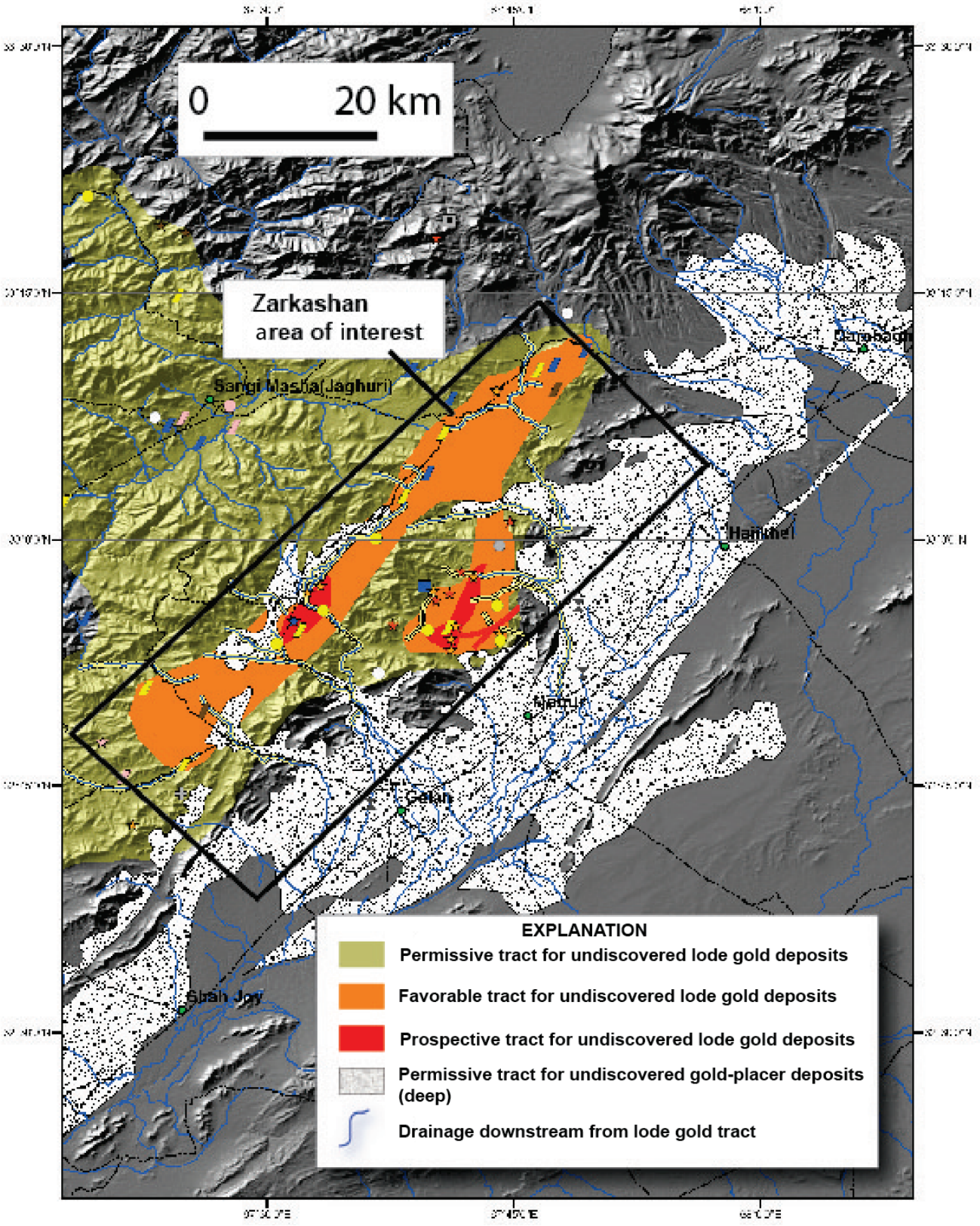

Figure 15A–30. Shaded relief map with assessment tracts permissive for gold placer deposits, from Peters and others (2007), showing locations of possible undiscovered deep gold placer deposits within and adjacent to the Zarkashan copper and gold area of interest. km, kilometer.

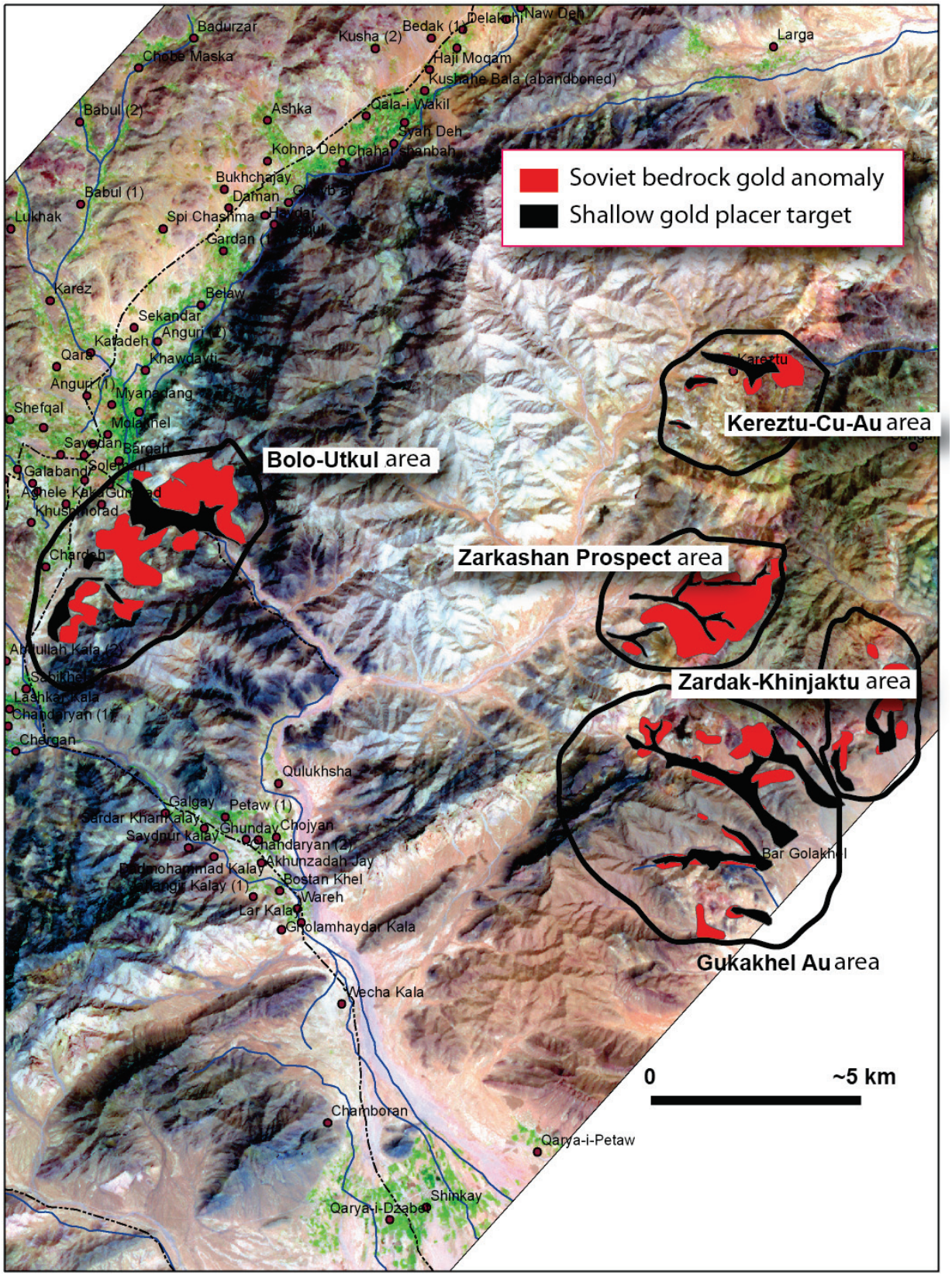

Figure 15A–31. Advanced Spaceborne Thermal Emission and Reflection radiometer image of the central parts of the Zarkashan copper and gold area of interest, showing major target areas, bedrock gold anomalous areas and potential for areas of shallow gold placer deposits. Green areas are vegetation in wet valleys. Au, gold; Cu, copper; km, kilometer. Small circles are village centers.

15A.15 References Cited

Abdullah, S., Chmyriov, V.M., Stazhilo–Alekseyev, K.F., Dronov, V.I., Gannan, P.J., Rossovskiy, L.N., Kafarskiy, A.Kh., and Malyarov, E.P., 1977, Mineral resources of Afghanistan (2d ed.): Kabul, Afghanistan, Republic of Afghanistan Geological and Mineral Survey, 419 p.

Afghanistan Geological and Mineral Survey, 1967, Geological structure of the Zarkashan gold deposit: Afghanistan Geological and Mineral Survey, 8 p.

Borozenets, N.I., 1972, Report on prospecting (scale 1:50,000) results obtained in the Anguri River's drainage area: [Afghanistan] Department of Geological and Mineral Survey, [unpaginated].

Cox, D.P., 1986a, Descriptive model of polymetallic veins, *in* Cox, D.P., and Singer, D.A., eds., Mineral deposit models: U.S. Geological Survey Bulletin 1693, p. 125.

Cox, D.P., 1986b, Descriptive model of porphyry Cu, *in* Cox, D.P., and Singer, D.A., eds., Mineral deposit models: U.S. Geological Survey Bulletin 1693, p. 77.

Cox, D.P., 1986c, Descriptive model of porphyry Cu-Au, *in* Cox, D.P., and Singer, D.A., eds., Mineral deposit models: U.S. Geological Survey Bulletin 1693, p. 110.

Cox, D.P., 1986d, Descriptive model of porphyry Cu-Mo, *in* Cox, D.P., and Singer, D.A., eds., Mineral deposit models: U.S. Geological Survey Bulletin 1693, p. 115

Cox, D.P., 1986e, Descriptive model of Zn-Pb skarn deposits, *in* Cox, D.P., and Singer, D.A., eds., Mineral deposit models: U.S. Geological Survey Bulletin 1693, p. 90.

Cox, D.P., and Singer, D.A., eds., 1986, Mineral deposit models: U.S. Geological Survey Bulletin 1693, 379 p., available at *http://pubs.usgs.gov/bul/b1693/*.

Cox, D.P., and Theodore, T.G., 1986, Descriptive model of Cu skarn deposits, *in* Cox, D.P., and Singer, D.A., eds., Mineral deposit models: U.S. Geological Survey Bulletin 1693, p. 86.

Doebrich, J .L., Ludington, S., Peters, S.G., Finn, C.A., Mars, J.C., Rowan, L.C., Stoesser, D.B., King, T.M., Eppinger, R.G., Wasy, A., and Younusi, M.O., 2007, Porphyry copper potential of Tethyan magmatic arcs of Afghanistan, *in* Andrew, C.J., and others (eds.), Digging deeper—Proceedings of the ninth biennial meeting of the Society for Geology Applied to Mineral Deposits, Dublin, Ireland, August 20–23, 2007: Society for Geology, p. 129–132.

Doebrich, J.L., and Wahl, R.R., comps., *with contributions by* Doebrich, J.L., Wahl, R.R., Ludington, S.D., Chirico, P.G., Wandrey, C.J., Bohannon, R.G., Orris, G.J., Bliss, J.D., and ____, 2006, Geologic and mineral resource map of Afghanistan: U.S. Geological Survey Open File Report 2006–1038, scale 1:850,000, available at *http://pubs.usgs.gov/of/2006/1038/*.

Douvgal, Yu.M., Chalyan, M.A., Nagalev, V.S., Demin, A.N., Vaulin, V.A., Belich, A.I., Sonin, I.I., Kononykhin, E.T., Zharikhin, K.G., Maksimov, N.P., Skvortsov, N.S., and Kharitonov, A.P., 1971, The geology and minerals of the south-eastern part of Central Afghanistan: [Afghanistan] Department of Geological and Mineral Survey, scale 1:200,000, [unpaginated].

Homilius, Joachim, 1968, Geoelectrical investigations in the gold placer deposit of Zarkashan, Afghanistan: Hannover, Germany, Bundesanstalt für Bodenforschung, [unpaginated].

Homilius, Joachim, 1970, Geoelektrische Untersuchungen im Goldseifenvorkommen Zarkasan/Afghanistan [Geoelectrical studies of gold placers in Zarkashan, Afghanistan]: Geologisches Jahrbuch, v. 88, p. 113–125.

John, D.A., Ayuso, R.A., Barton, M.D., Blakely, R.J., Bodnar, R.J., Dilles, J.H., Gray, Floyd, Graybeal, F.T., Mars, J.C., McPhee, D.K., Seal, R.R., Taylor, R.D., and Vikre, P.G., 2010, Porphyry copper deposit model, chap. B *of* Mineral deposit models for resource assessment: U.S. Geological Survey Scientific Investigations Report 2010–5070, 169 p.

Khananov, R.M., Plotnikov, G.I., Bayazitov, R.A., Zamarayev, G.N., Trifonoy, A.I., and Sayanin, V.I., 1967, Report on the results of revisory evaluation of copper, lead, and gold deposits and occurrences carried out in 1965–1966: Department of Geological and Mineral Survey, [unpaginated].

Kononykhin, E.T., Zharikhin, K.G., Maksimov, N.P., Skvortsov, N.S., and Kharitonov, A.P., 1971, The geology and minerals of the south-eastern part of Central Afghanistan—Report on the results of prospecting and survey operations (scale 1:200,000) carried out in 1967–1970: [Afghanistan] Department of Geological and Mineral Survey, [unpaginated].

Kotov, A.Y., and others, 1971, Report on prospecting and exploratory work at Zarkashan during 1967–1970: [Afghanistan] Department of Geological and Mineral Survey, [unpaginated].

Mecheryakov, Y.P, and Sayapin, V.P., 1968, Geological map of the area of Zarkashan-Anguri gold deposits, in Mecheryakov, Y.P, and Sayapin, V.P., Report about results of geological prospecting works at the Zarkashan deposit and placer in 1967 [and project of geological exploration for 1968]: [Afghanistan] Ministry of Mines and Industries report no. R0657, one sheet, scale 1:50,000. [Prepared by V/O Technoexport U.S.S.R. under contract no. 1378.]Kovalenko, A.G., and others, 1971, Zarkashan gold deposit: [Afghanistan] Department of Geological and Mineral Survey, [unpaginated].

Ludington, Steve, Orris, G .J., Bolm, K.S., Peters, S.G., and the U.S. Geological Survey-Afghanistan Ministry of Mines and Industry Joint Mineral Resource Assessment Team, 2007, Preliminary mineral resource assessment of selected mineral deposit types in Afghanistan: U.S. Geological Survey Open-File Report 2007–1005, 44 p., accessed June 23, 2011, at *http://pubs.usgs.gov/of/2007/1005/*.

Mars, J.C., and Rowan, L.C., 2007, Mapping phyllic and argillic-altered rocks in southeastern Afghanistan using advanced spaceborne thermal emission and reflection radiometer (ASTER) data: U.S. Geological Survey Open-File Report 2007–1006, 1 sheet, accessed June 23, 2011, at *http://pubs.usgs.gov/of/2007/1006/*.

Meshcheryakov, E.P., and Borozenets, N.I., 1970, Report on the results of geological exploration carried out within the Mokur ore field in 1969: [Afghanistan] Department of Geological and Mineral Survey, [unpaginated].

Metal Mining Agency of Japan, 1998, Mineral resources map of Asia: Metal Mining Agency of Japan, 1:1,000,000,000-scale, 43-p. text.

Morris, H.T., 1986, Descriptive model of polymetallic replacement deposits, *in* Cox, D.P., and Singer, D.A., eds., Mineral deposit models: U.S. Geological Survey Bulletin 1693, p. 99.

Mosier, D.L., and Menzie, W.D., 1986, Descriptive model of Fe skarn deposits, *in* Cox, D.P., and Singer, D.A., eds., Mineral deposit models: U.S. Geological Survey Bulletin 1693, p. 94.

Mosier, D.L., Morris, H.T., and Singer, D.A., 1986a, Grade and tonnage model polymetallic replacement deposits, *in* Cox, D.P., and Singer, D.A. eds., Mineral deposit models: U.S. Geological Survey Bulletin 1693, p. 101–104.

Mosier, D.L., Singer, D.A., and Berger, B.R., 1986b, Descriptive model of Comstock epithermal veins, *in* Cox, D.P., and Singer, D.A., eds., Mineral deposit models: U.S. Geological Survey Bulletin 1693, p. 150.

Orris, G.J., and Bliss, J.D., 2002, Mines and mineral occurrences of Afghanistan: U.S. Geological Survey Open-File Report 2002–110, 95 p., accessed September 1, 2006, at *http://geopubs.wr.usgs.gov/open-file/of02-110/*.

Peters, S.G., Ludington, S.D., Orris, G.J., Sutphin, D.M., Bliss, J.D., and Rytuba, J.J., eds., and the U.S. Geological Survey-Afghanistan Ministry of Mines Joint Mineral Resource Assessment Team, 2007, Preliminary non-fuel mineral resource assessment of Afghanistan: U.S. Geological Survey Open-File Report 2007–1214, 810 p., 1 CD–ROM. (Also available at *http://pubs.usgs.gov/of/2007/1214/*.)

Peters, S.G., Stettner, W.R., Masonic, L.M., and Moran, T.W., comps., 2011, Geologic map of the Zarkashan-Anguri copper and gold deposits, Ghazni Province, Afghanistan, modified from the 1968 original map compilation of E.P. Meshcheryakov and V.P. Sayapin: U.S. Geological Survey Open-File Report 2011–1212, one sheet, scale 1:40,000, available at *http://pubs.usgs.gov/of/2011/1212/*.

Singer, D.A., 1986, Grade and tonnage model of porphyry Cu, skarn-related deposits, *in* Cox, D.P., and Singer, D.A., eds., Mineral deposit models: U.S. Geological Survey Bulletin 1693, p. 82.

Singer, D.A., Berger, V.I., and Moring, B.C., 2008, Porphyry copper deposits of the world—Database, map, and grade and tonnage models: U.S. Geological Survey Open-File Report 2008–1155, accessed June 23, 2011, at *http://pubs.usgs.gov/of/2008/1155/*.

Sweeney, R.E., Kucks, R.P., Hill, P.L, and Finn, C.A., 2006, Aeromagnetic and gravity surveys in Afghanistan—A web site for distribution of data: U.S. Geological Survey Open File Report 2006–1204, accessed June 23, 2011, at *http://pubs.usgs.gov/of/2006/1204/*.

Theodore, Ted, 2010, Afghanistan petrology: [Afghanistan] Department of Geological and Mineral Survey, August, 3 vols.

United Nations Economic and Social Commission for Asia and the Pacific, 1995, Atlas of mineral resources of the ESCAP region—Geology and mineral resources of Afghanistan: United Nations Economic and Social Commission for Asia and the Pacific, 150 p. [Available from the National Technical Information Service, Springfield, Va., as NTIS Report UN–0561.]

U.S. Department of Defense Task Force for Business and Stability Operations, 2010, Mineral Resource Team 2010 activities summary, 49 p., accessed June 23, 2011, at *http://tfbso.defense.gov/www/TFBSO_AFGHAN_MINERALS.pdf*.